

ULQ2 (Ultra-Low Q₂)

Toshimi Suda
Research Center for Electron-Photon Science
Tohoku University, Sendai, JAPAN

on behalf of the ULQ2 collaboration

Low- q electron-scattering activities in Japan



charge radii of proton and deuteron

$E_e = 10 - 60 \text{ MeV}$
 $\theta_e = 30 - 150 \text{ deg.}$
 $\Rightarrow Q^2 = 3 \times 10^{-5} - 0.013 (\text{GeV}/c)^2$

e-scattering of online-produced exotic nuclei ($\sim 10^8/\text{sec}$)

$E_e = 150 - 300 \text{ MeV}$
 $\theta_e = 30 - 60 \text{ deg.}$
 $\Rightarrow q = 80 - 300 \text{ MeV}/c$
 $Q^2 = 0.006 - 0.09 (\text{GeV}/c)^2$

Low- q electron-scattering activities in Japan



charge radii of proton and deuteron

$E_e = 10 - 60 \text{ MeV}$

$\theta_e = 30 - 150 \text{ deg.}$

$\Rightarrow Q^2 = 3 \times 10^{-5} - 0.013 (\text{GeV}/c)^2$

e-scattering of online-produced exotic nuclei ($\sim 10^8/\text{sec}$)

$E_e = 150 - 300 \text{ MeV}$

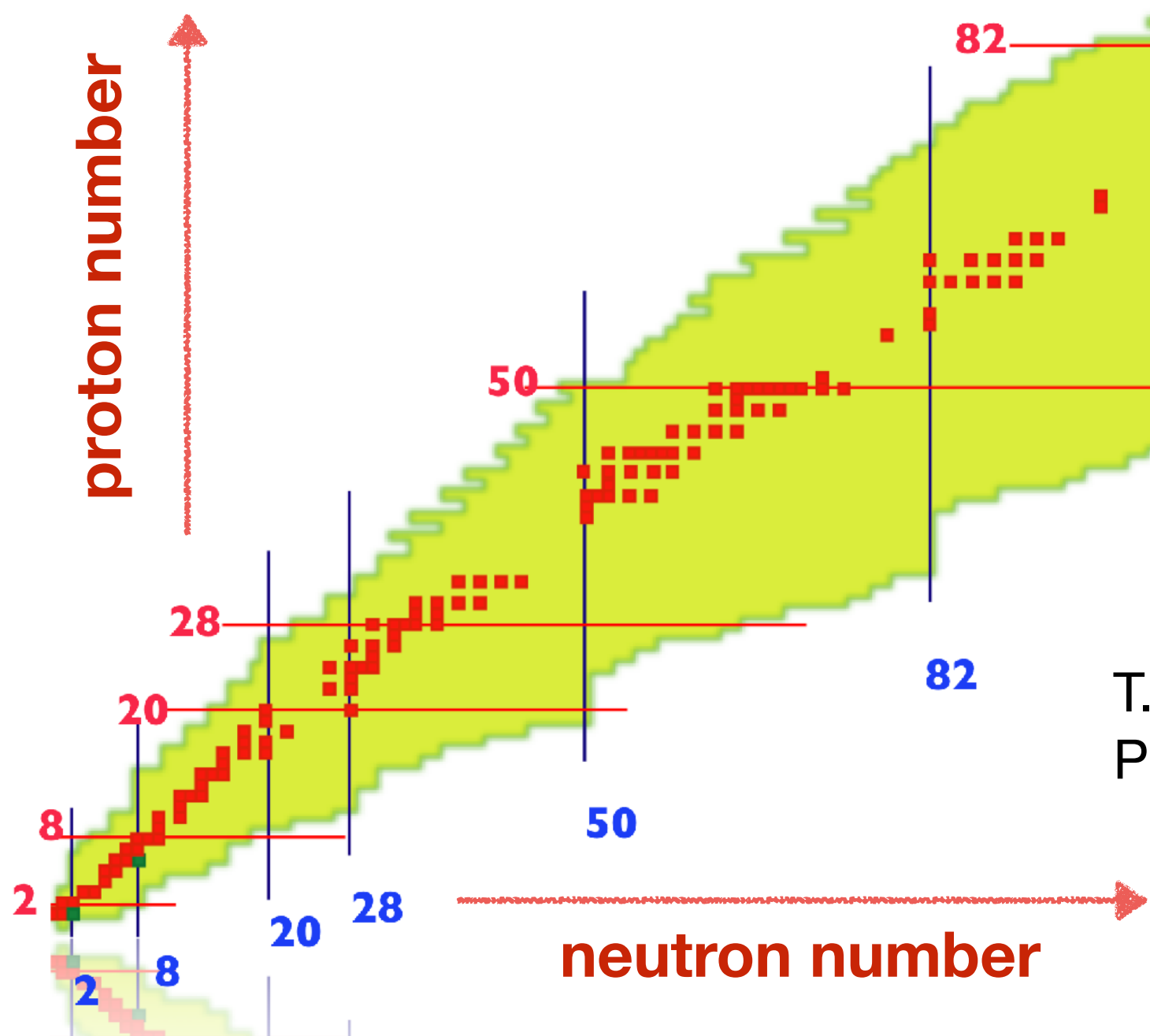
$\theta_e = 30 - 60 \text{ deg.}$

$\Rightarrow q = 80 - 300 \text{ MeV}/c$

$Q^2 = 0.006 - 0.09 (\text{GeV}/c)^2$

Nuclei ever studied with electron scattering

- strictly limited to stable nuclei (+ long-lived)
- never applied for exotic nuclei (short-lived)



T. S. and H. Simon,
Prog. Part. Nucl. Phys. 96 (2017) 1-31.

First e-scat. paper for online-produced unstable nuclei

PHYSICAL REVIEW LETTERS 131, 092502 (2023)

Editors' Suggestion

Featured in Physics

First Observation of Electron Scattering from Online-Produced Radioactive Target

K. Tsukada^{1,2}, Y. Abe,² A. Enokizono,^{2,3} T. Goke,⁴ M. Hara,² Y. Honda,^{2,4} T. Hori,² S. Ichikawa,^{2,*} Y. Ito,¹ K. Kurita^{1,3}, C. Legris^{1,4}, Y. Maehara,¹ T. Ohnishi,² R. Ogawara,^{1,2} T. Suda^{1,2,4}, T. Tamae,⁴ M. Wakasugi,^{1,2} M. Watanabe,² and H. Wauke^{2,4}

¹Institute for Chemical Research, Kyoto University, Uji, Kyoto 611-0011, Japan

²Nishina Center for Accelerator-Based Science, RIKEN, Wako, Saitama 351-0198, Japan

³Department of Physics, Rikkyo University, Toshima, Tokyo 171-8501, Japan

⁴Research Center for Electron Photon Science, Tohoku University, Sendai, Miyagi 982-0826, Japan



(Received 7 March 2023; accepted 21 June 2023; published 30 August 2023)

We successfully performed electron scattering off unstable nuclei which were produced online from the photofission of uranium. The target ^{137}Cs ions were trapped with a new target-forming technique that makes a high-density stationary target from a small number of ions by confining them in an electron storage ring. After developments of target generation and transportation systems and the beam stacking method to increase the ion beam intensity up to approximately 2×10^7 ions per pulse beam, an average luminosity of $0.9 \times 10^{26} \text{ cm}^{-2} \text{ s}^{-1}$ was achieved for ^{137}Cs . The obtained angular distribution of elastically scattered electrons is consistent with a calculation. This success marks the realization of the anticipated femtoscope which clarifies the structures of exotic and short-lived unstable nuclei.

DOI: [10.1103/PhysRevLett.131.092502](https://doi.org/10.1103/PhysRevLett.131.092502)

Electron scattering provides a long-awaited view of unstable nuclei

Nuclear reactions produce a plethora of short-lived artificial isotopes. Figuring out what they look like has been a challenge.

The cartoon picture of an atomic nucleus looks kind of like the inside of a gumball machine that dispenses only two flavors: protons and neutrons, evenly mixed in a compact, spherical cluster.

That's not generally what real nuclei look like. Neutron-rich lead-208, for example, has a thick skin of neutrons encasing its proton-endowed core (see PHYSICS TODAY, July 2021, page 12). Some nuclei are flattened, and some are elongated. Some are even pear shaped.

The more unstable a nucleus, the

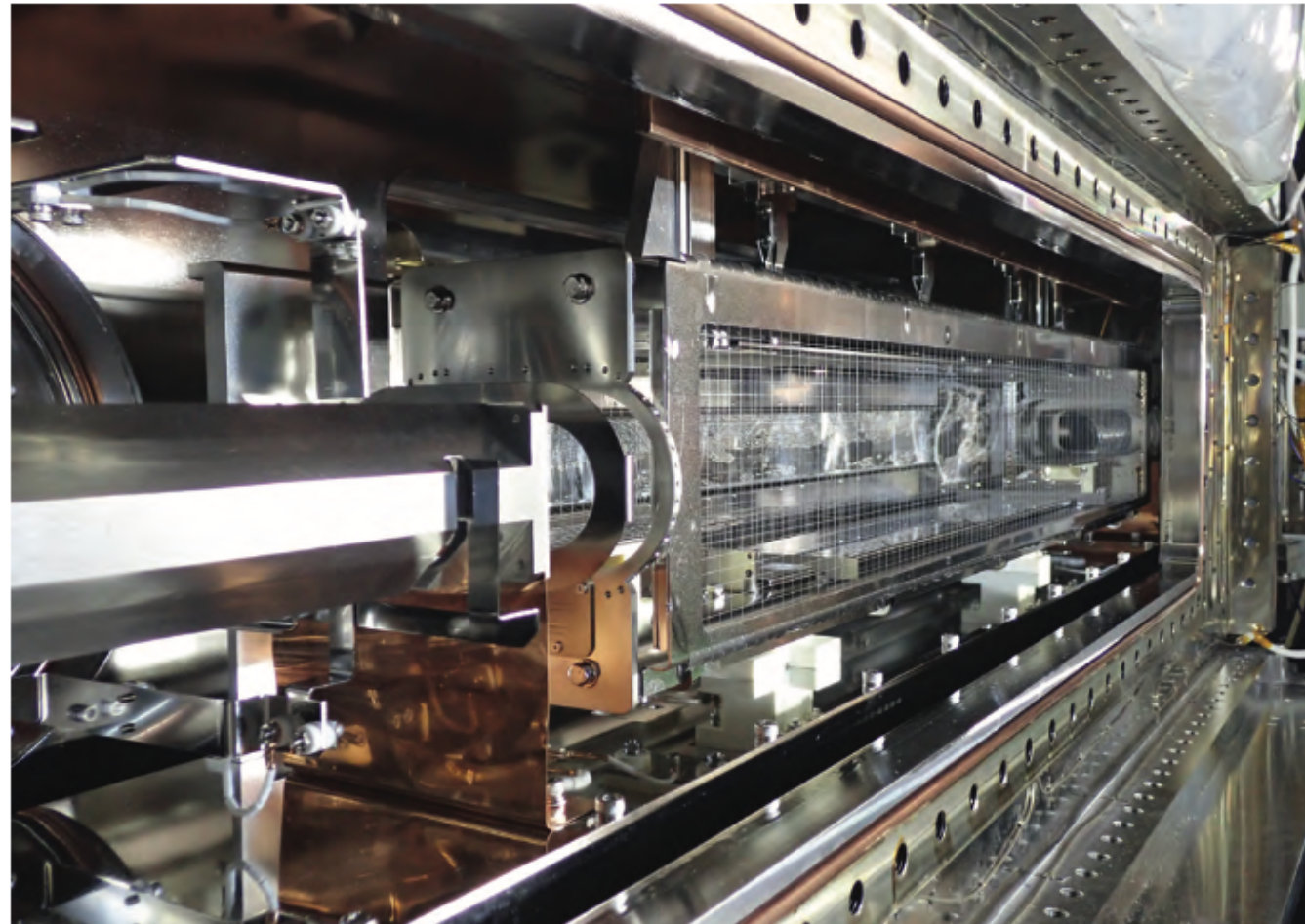
stranger the structures it can adopt. Short-lived nuclei might form bubble structures with depleted central density, or they might have a valence nucleon or two that form a halo around a compact central core. (See the article by Filomena Nunes, PHYSICS TODAY, May 2021, page 34.) Frustratingly, though, those exotic structures are hard to experimentally confirm, because the gold standard for probing nuclear structure—electron scattering—has been off limits to short-lived nuclei.

That could change soon. Kyo Tsukada

and colleagues, working at RIKEN's Radioactive Isotope Beam Factory (RIBF) in Wako, Japan, have performed the first electron-scattering experiment on unstable nuclei produced on the fly in a nuclear reaction.¹ Their isotope of choice, cesium-137, has a half-life of 30 years. It's not so exotic that the researchers expected—or found—anything unusual about its structure. But the technique they used is applicable to shorter-lived nuclei, so more experiments are on the way.

Backscatter

Probing nuclei through particle scattering dates back to the discovery of the nucleus itself, in 1911, when Ernest



01 November 2023 22:46:08

FIGURE 1. RADIOACTIVE IONS too short-lived to be made into a solid target can nevertheless be trapped in an electron beam. The beam itself traps the ions in two dimensions; the cage of thin wire electrodes creates an electric potential that traps them in the third. (Courtesy of Tetsuya Ohnishi.)

Electron scattering provides a long-awaited view of unstable nuclei

Nuclear reactions produce a plethora of short-lived artificial isotopes. Figuring out what they look like has been a challenge.

The cartoon picture of an atomic nucleus looks kind of like the inside of a gumball machine that dispenses only two flavors: protons and neutrons, evenly mixed in a compact, spherical cluster.

That's not generally what real nuclei look like. Neutron-rich lead-208, for example, has a thick skin of neutrons encasing its proton-endowed core (see PHYSICS TODAY, July 2021, page 12). Some nuclei are flattened, and some are elongated. Some are even pear shaped.

The more unstable a nucleus, the

stranger the structures it can adopt. Short-lived nuclei might form bubble structures with depleted central density, or they might have a valence nucleon or two that form a halo around a compact central core. (See the article by Filomena Nunes, PHYSICS TODAY, May 2021, page 34.) Frustratingly, though, those exotic structures are hard to experimentally confirm, because the gold standard for probing nuclear structure—electron scattering—has been off limits to short-lived nuclei.

That could change soon. Kyo Tsukada

and colleagues working at RIKEN's Ra-

di-

in

fir

ur

a

ch

ye

er

us

ni

liv

th

Ba

Pr

in

nu

Frustratingly, though, those exotic structures are hard to experimentally confirm, because the gold standard for probing nuclear structure—electron scattering—has been off limits to short-lived nuclei.



FIGURE 1. RADIOACTIVE IONS too short-lived to be made into a solid target can nevertheless be trapped in an electron beam. The beam itself traps the ions in two dimensions; the cage of thin wire electrodes creates an electric potential that traps them in the third. (Courtesy of Tetsuya Ohnishi.)

RIKEN SCRIT Electron Scattering Facility

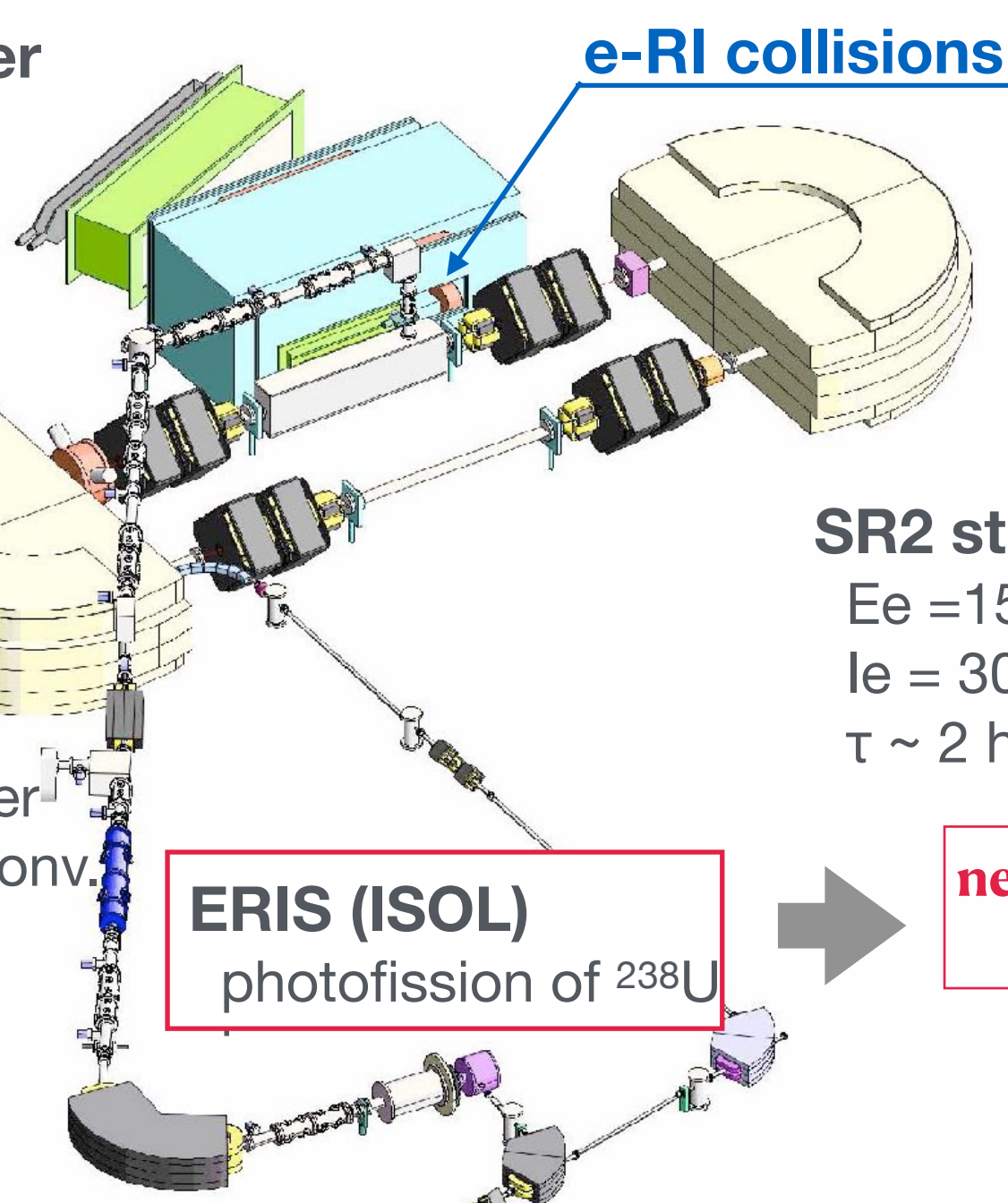
WiSES spectrometer

$\Delta\Omega \sim 90$ mSr

$\theta = 30 - 60^\circ$

$\Delta p/p \sim 10^{-3}$

long target accept.



SR2 storage ring

$E_e = 150 - 700$ MeV

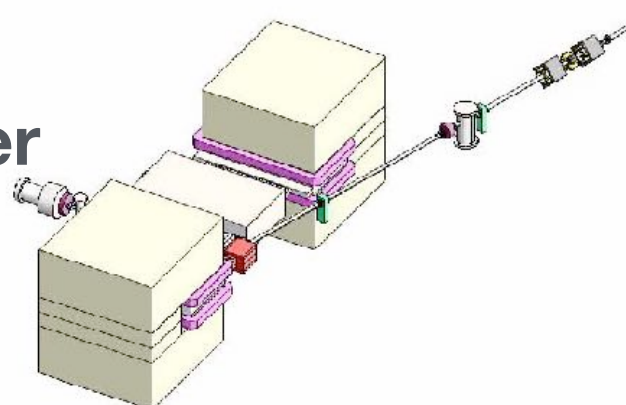
$I_e = 300$ mA

$\tau \sim 2$ hours

**neutron-rich nuclei
by $\gamma + {}^{238}\text{U}$**

Injector + ISOL driver

150 MeV Microtron



SCRIT

Nucl. Instrum. Methods A532 (2004) 216.

Phys. Rev. Lett. 100 (2008) 164801.

Phys. Rev. Lett. 102 (2009) 102501.

SCRIT Facility : Nucl. Instrum. Method B317 (2013) 668.

ERIS : Nucl. Instrum. Method B317 (2013) 357.

FRAC : Rev. Sci. Instrum. 89 (2018) 095107.

RIKEN SCRIT facility

*The world's first electron-scattering facility
dedicated for short-lived exotic nuclei*

Electron Ring
(SCRIT equipped)

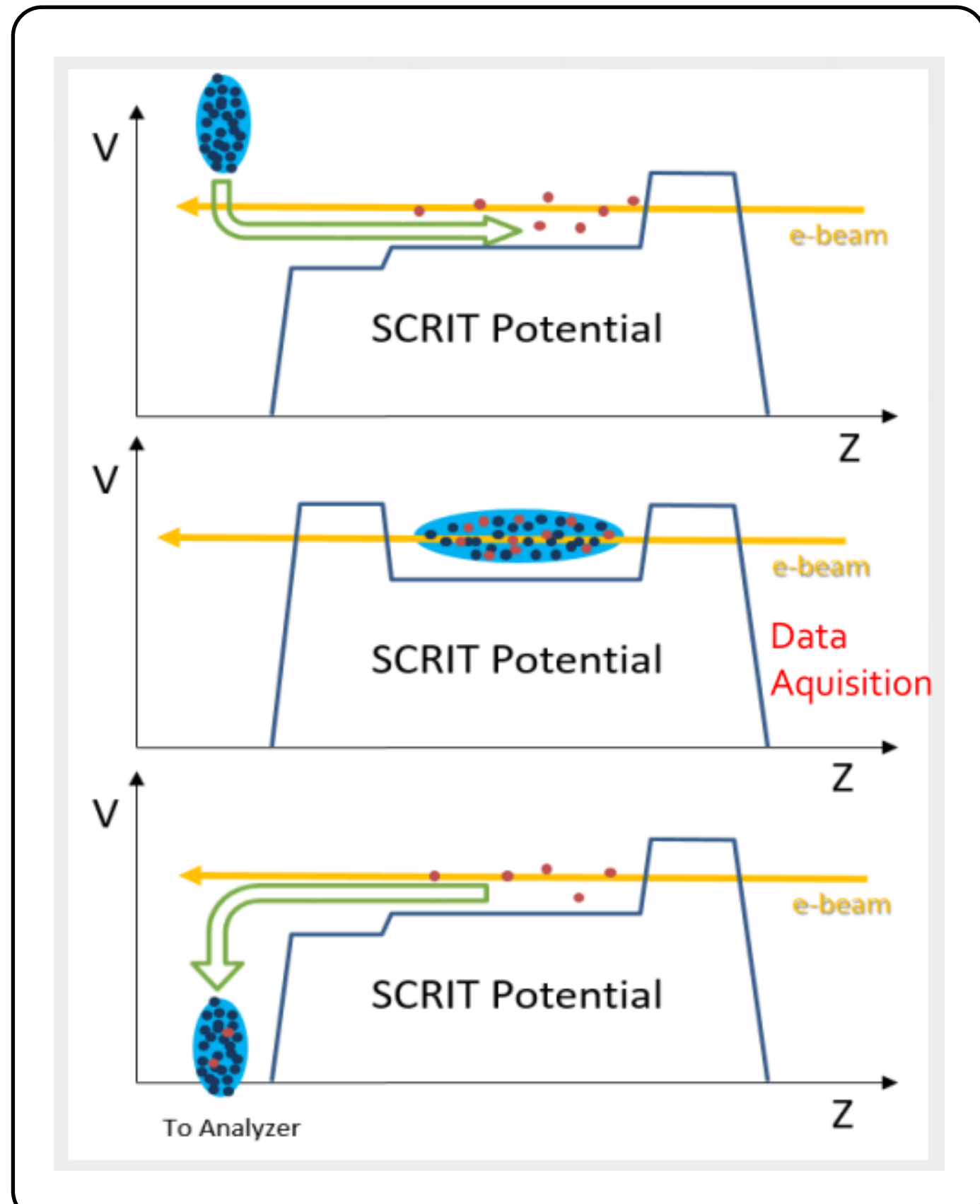
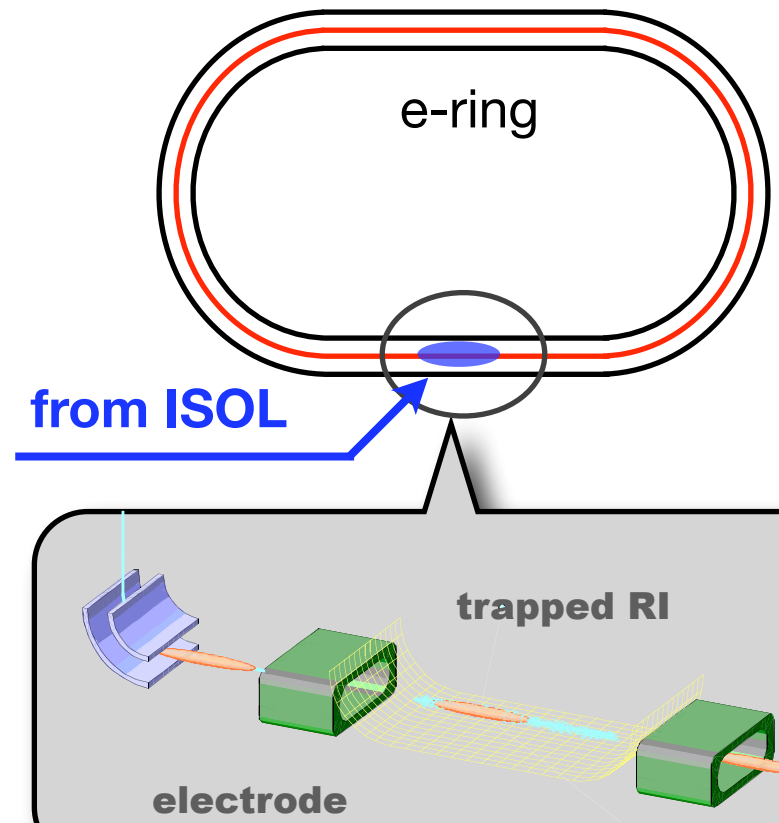
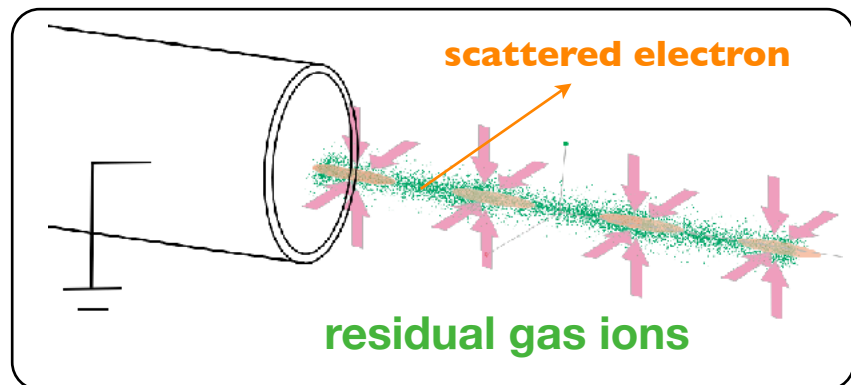
WiSES
(Window-frame Spectrometer
for Electron Scattering)

SCRIT (Self-Confining RI Ion Target)

Idea : “ion trapping” at SR facilities.

ionized residual gases are trapped by the circulating electron beam

ill problem of e-storage rings



Luminosities for e-scattering

	E _e	N _{beam}	target thickness	L
Hofstadter's era (1950s)	150 MeV	~1nA (~ 10^9 /s)	~ 10^{19} /cm ²	~ 10^{28} /cm ² /s
JLAB	12 GeV	~100μA (~ 10^{14} /s)	~ 10^{22} /cm ²	~ 10^{36} /cm ² /s

Luminosities for e-scattering

	E_e	N_{beam}	target thickness	L
Hofstadter's era (1950s)	150 MeV	$\sim 1\text{nA}$ $(\sim 10^9 / \text{s})$	$\sim 10^{19} / \text{cm}^2$	$\sim 10^{28} / \text{cm}^2/\text{s}$
JLAB	12 GeV	$\sim 100\mu\text{A}$ $(\sim 10^{14} / \text{s})$	$\sim 10^{22} / \text{cm}^2$	$\sim 10^{36} / \text{cm}^2/\text{s}$
SCRIT	150-300 MeV	300 mA $(\sim 10^{18} / \text{s})$	$\sim 10^9 / \text{cm}^2$	$\sim 10^{27} / \text{cm}^2/\text{s}$

Luminosities for e-scattering

	E_e	N_{beam}	target thickness	L
Hofstadter's era (1950s)	150 MeV	$\sim 1\text{nA}$ $(\sim 10^9 / \text{s})$	$\sim 10^{19} / \text{cm}^2$	$\sim 10^{28} / \text{cm}^2/\text{s}$
JLAB	12 GeV	$\sim 100\mu\text{A}$ $(\sim 10^{14} / \text{s})$	$\sim 10^{22} / \text{cm}^2$	$\sim 10^{36} / \text{cm}^2/\text{s}$
SCRIT	150-300 MeV	300 mA $(\sim 10^{18} / \text{s})$	$\sim 10^9 / \text{cm}^2$	$\sim 10^{27} / \text{cm}^2/\text{s}$

$\sim 10^7$ trapped ions
in e-beam of
 $\sim 1 \text{ mm}^2$

Luminosities for e-scattering

	E_e	N_{beam}	target thickness	L
Hofstadter's era (1950s)	150 MeV	$\sim 1\text{nA}$ $(\sim 10^9 / \text{s})$	$\sim 10^{19} / \text{cm}^2$	$\sim 10^{28} / \text{cm}^2/\text{s}$
JLAB	12 GeV	$\sim 100\mu\text{A}$ $(\sim 10^{14} / \text{s})$	$\sim 10^{22} / \text{cm}^2$	$\sim 10^{36} / \text{cm}^2/\text{s}$
SCRIT	150-300 MeV	300 mA $(\sim 10^{18} / \text{s})$	$\sim 10^9 / \text{cm}^2$	$\sim 10^{27} / \text{cm}^2/\text{s}$

~10⁷ trapped ions
in e-beam of
~1 mm²

required target thickness ~ 10⁻¹⁰ !!

Low- q electron-scattering activities in Japan



charge radii of proton and deuteron

$E_e = 10 - 60 \text{ MeV}$
 $\theta_e = 30 - 150 \text{ deg.}$
 $\Rightarrow Q^2 = 3 \times 10^{-5} - 0.013 (\text{GeV}/c)^2$

e-scattering of online-produced exotic nuclei ($\sim 10^8/\text{sec}$)

$E_e = 150 - 300 \text{ MeV}$
 $\theta_e = 30 - 60 \text{ deg.}$
 $\Rightarrow q = 80 - 300 \text{ MeV}/c$
 $Q^2 = 0.006 - 0.09 (\text{GeV}/c)^2$

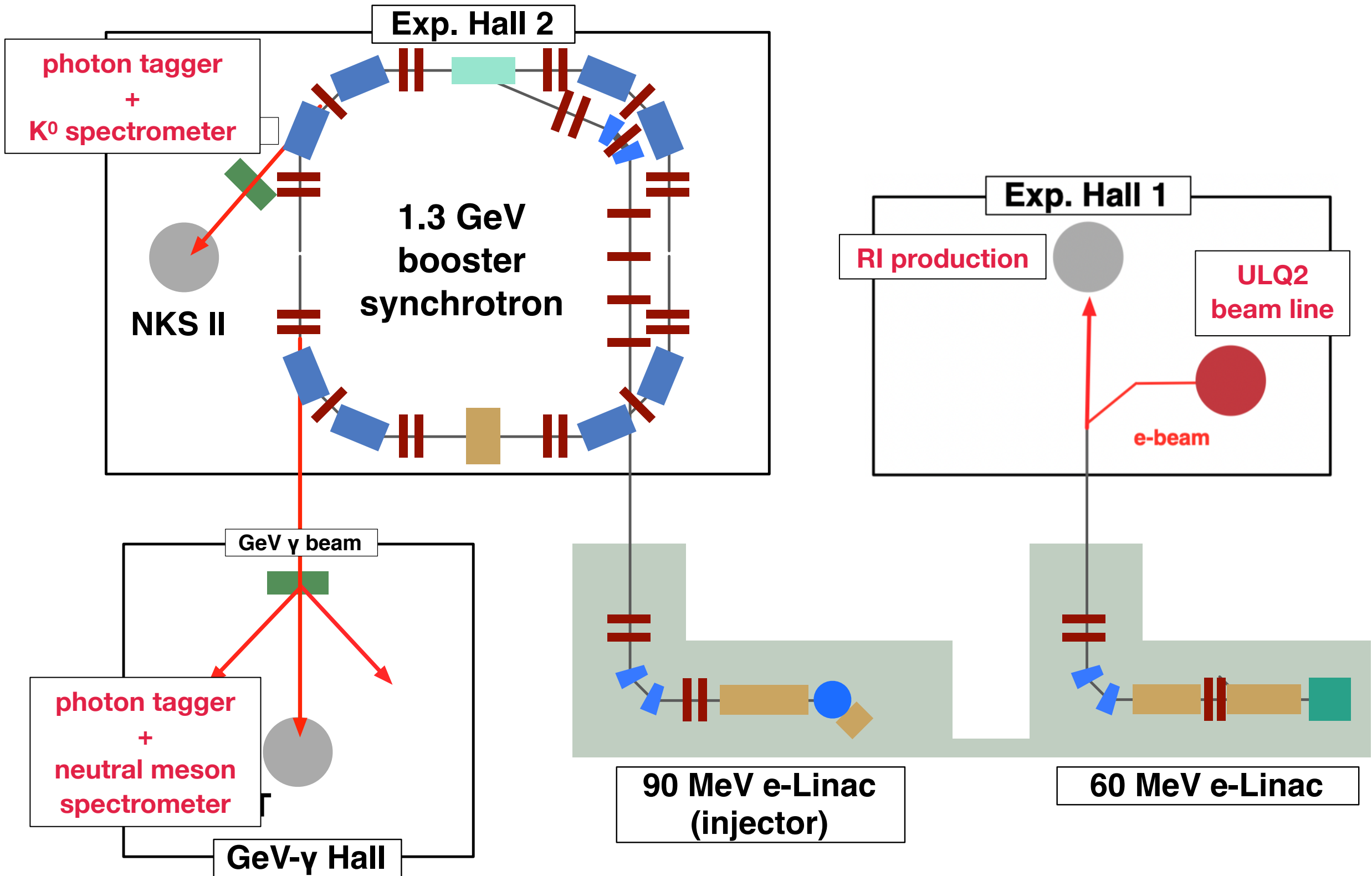
- 1) Tohoku ULQ2 facility**
- 2) ULQ2 physics program and current status**
- 3) Summary**



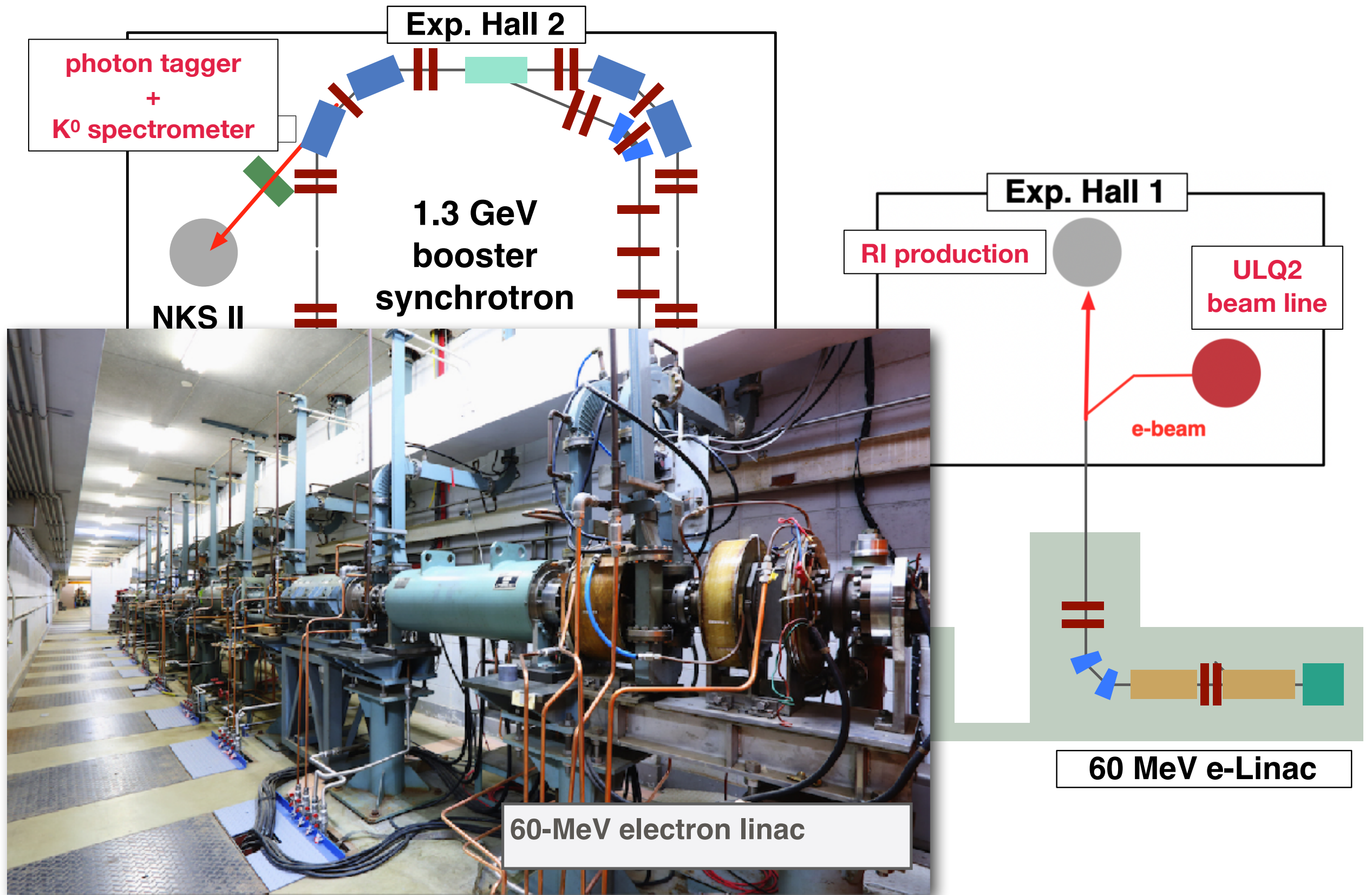
Sendai

Research Center for Electron-Photon Science
Tohoku University

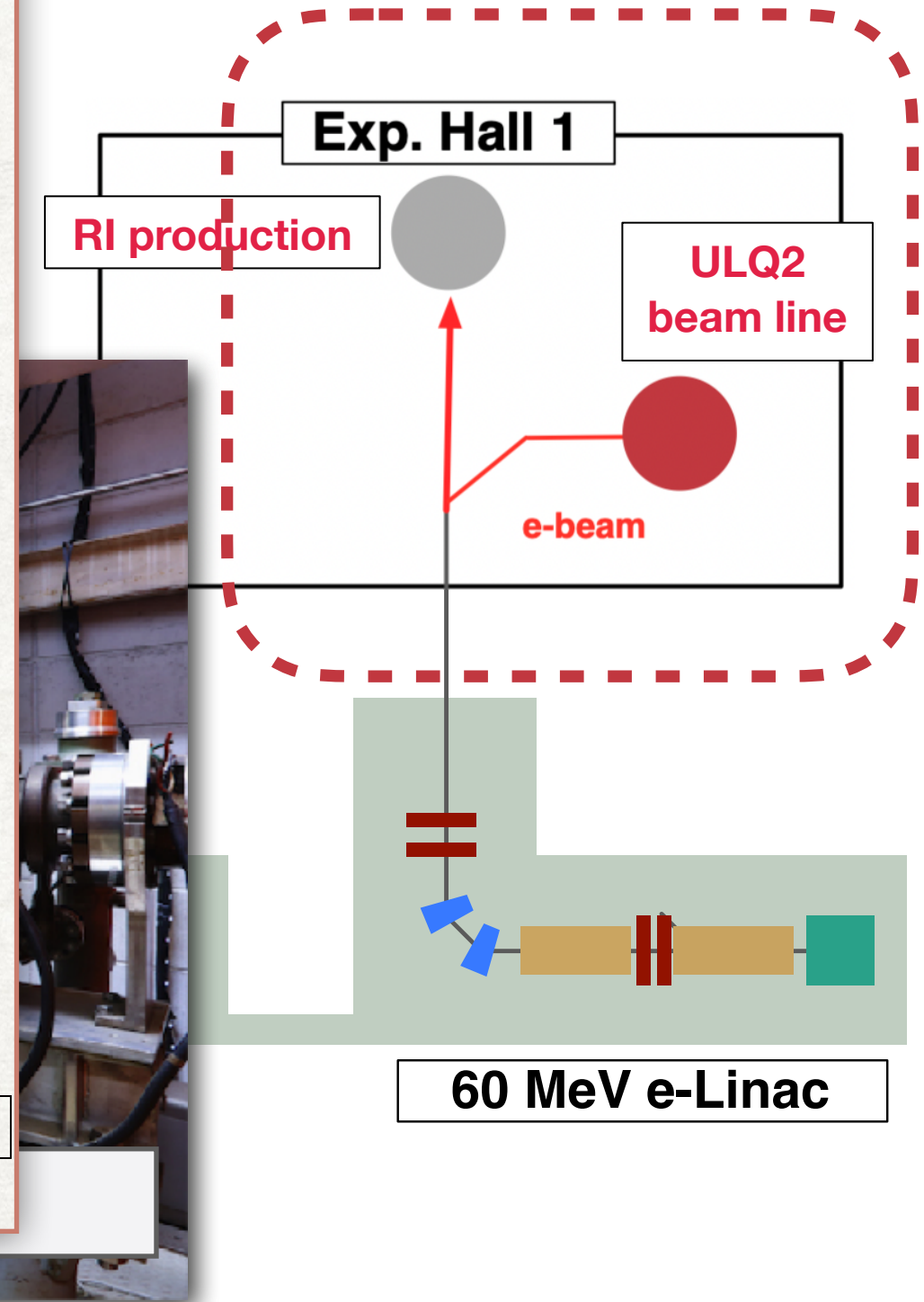
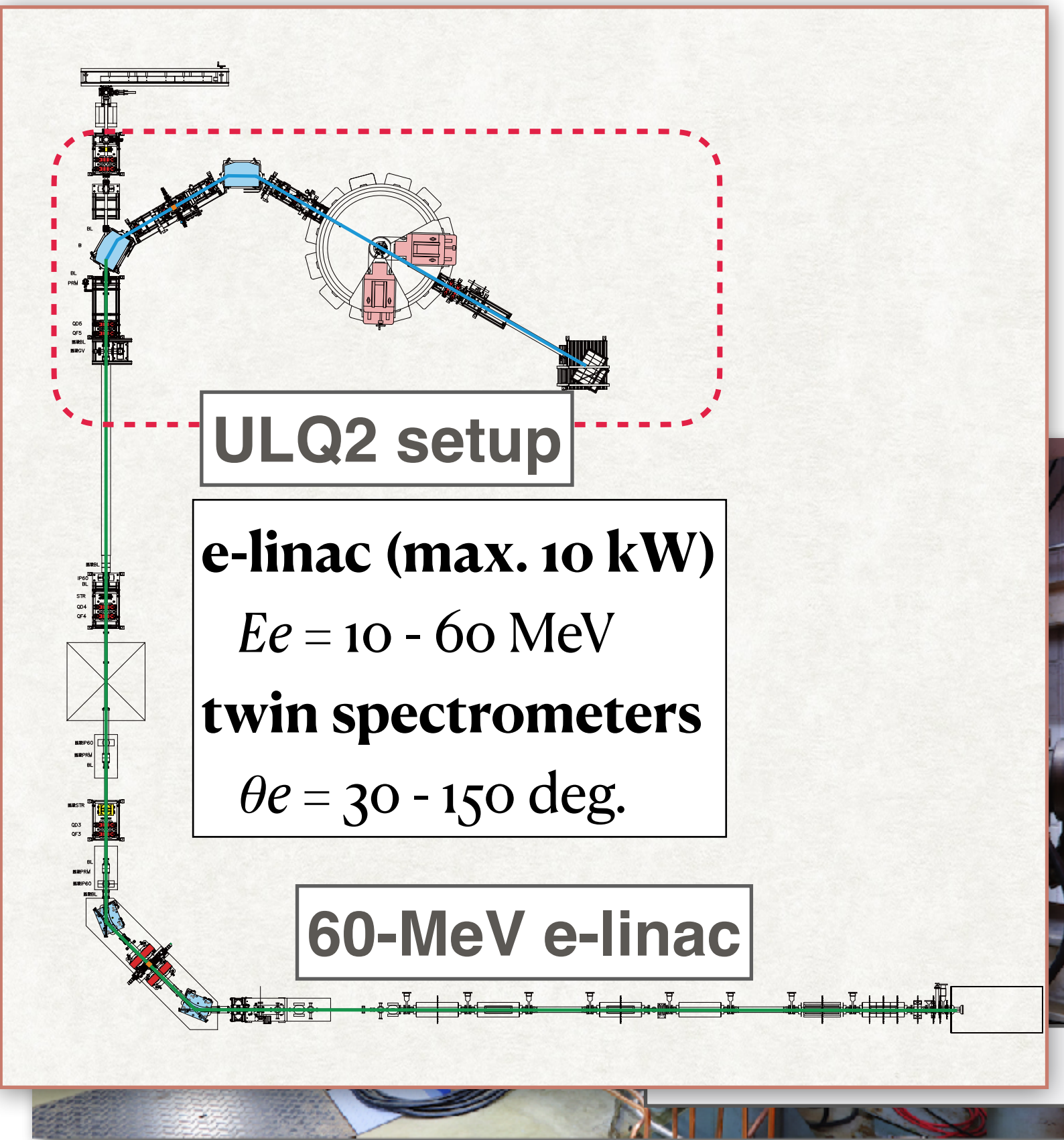
Tohoku University Research Center for ELectron-PHoton Science (ELPH)



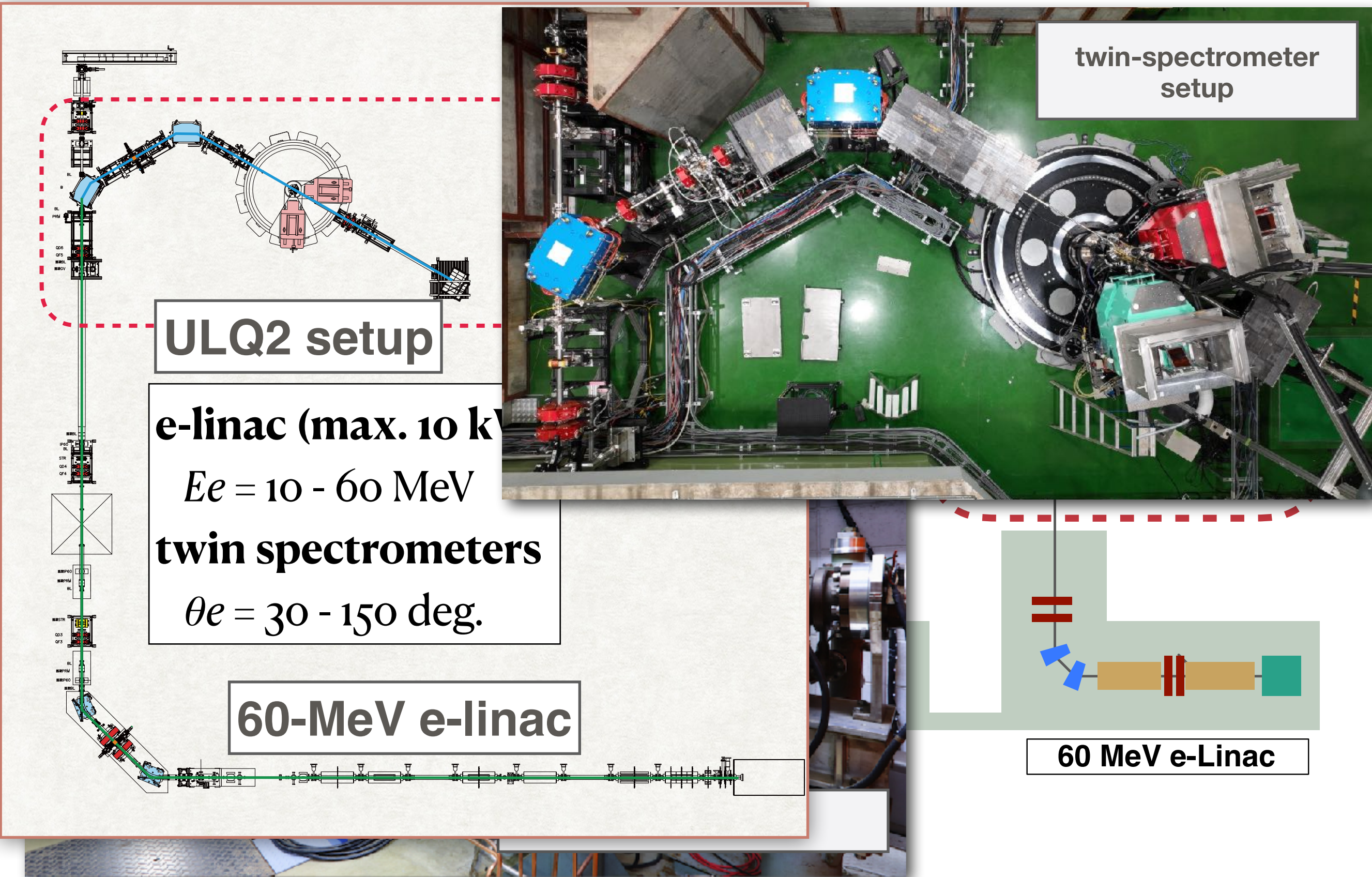
Tohoku University Research Center for ELectron-PHoton Science (ELPH)



Tohoku University Research Center for ELectrон-PHoton Science (ELPH)



Tohoku University Research Center for ELectron-PHoton Science (ELPH)



60 MeV electron linac

$E_e = 10 - 60 \text{ MeV}$

(absolute 10^{-3})

$\Delta E/E = 0.6 \times 10^{-4}$

beam size $\sim 0.6 \text{ mm}$ on target

$I_e = 1 \text{ nA} - 1 \mu\text{A}$

duty factor = 10^{-3}

ULQ2 twin-spectrometer setup

$\Delta p/p = 5.6 \times 10^{-3}$

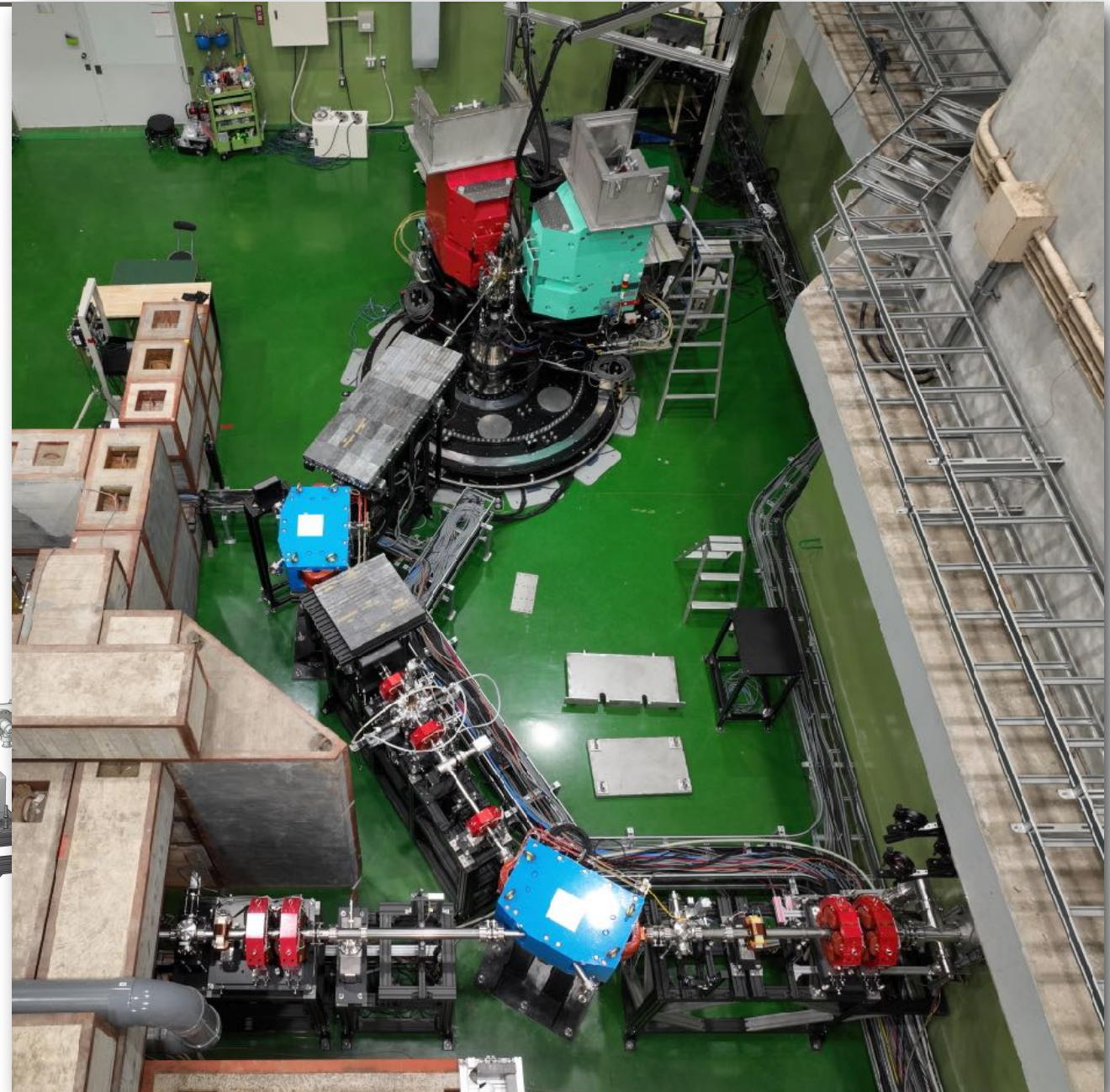
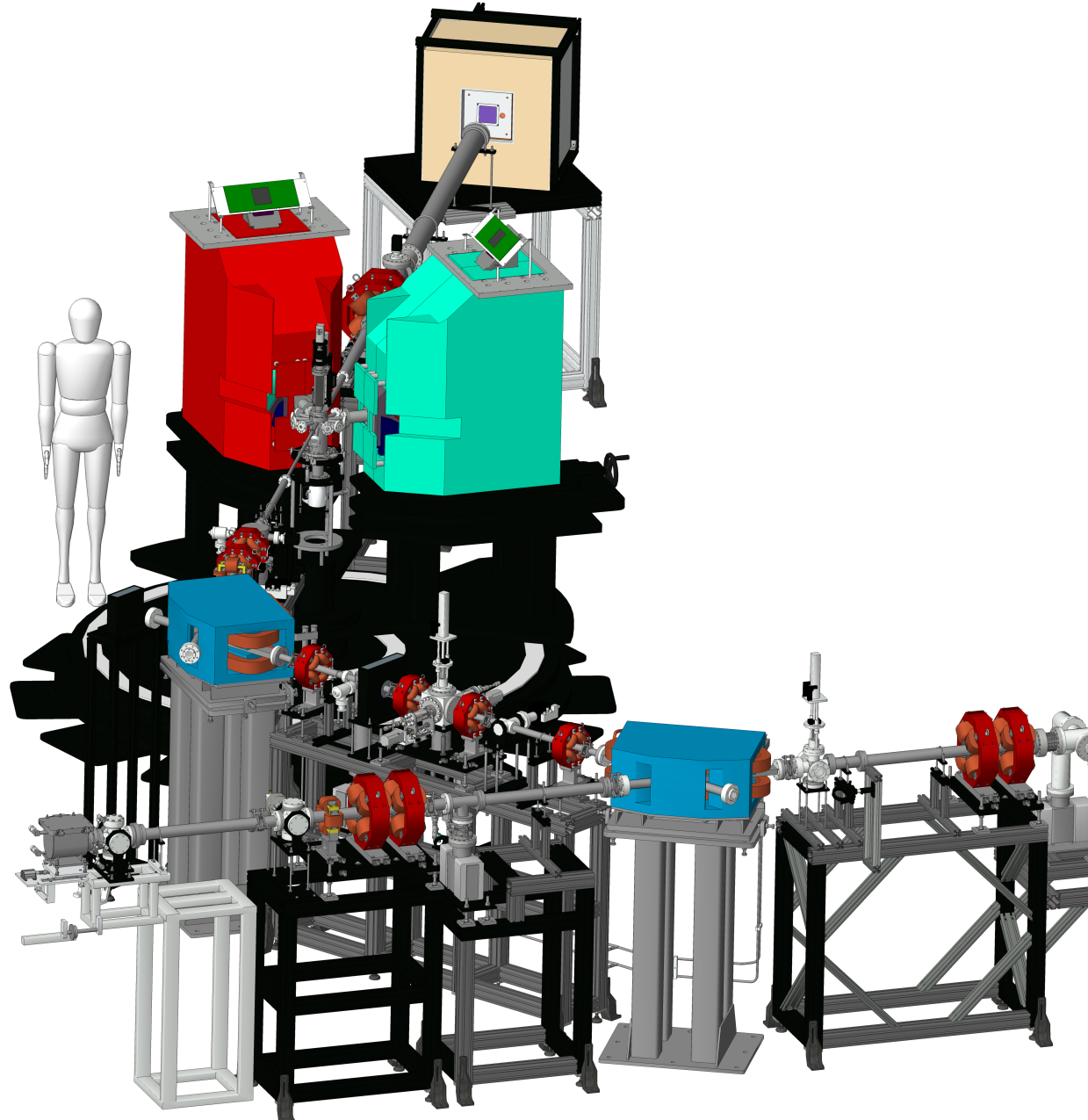
$\Delta\Omega = 6 \text{ mSr}$

$\theta = 30 - 150 \text{ deg.}$

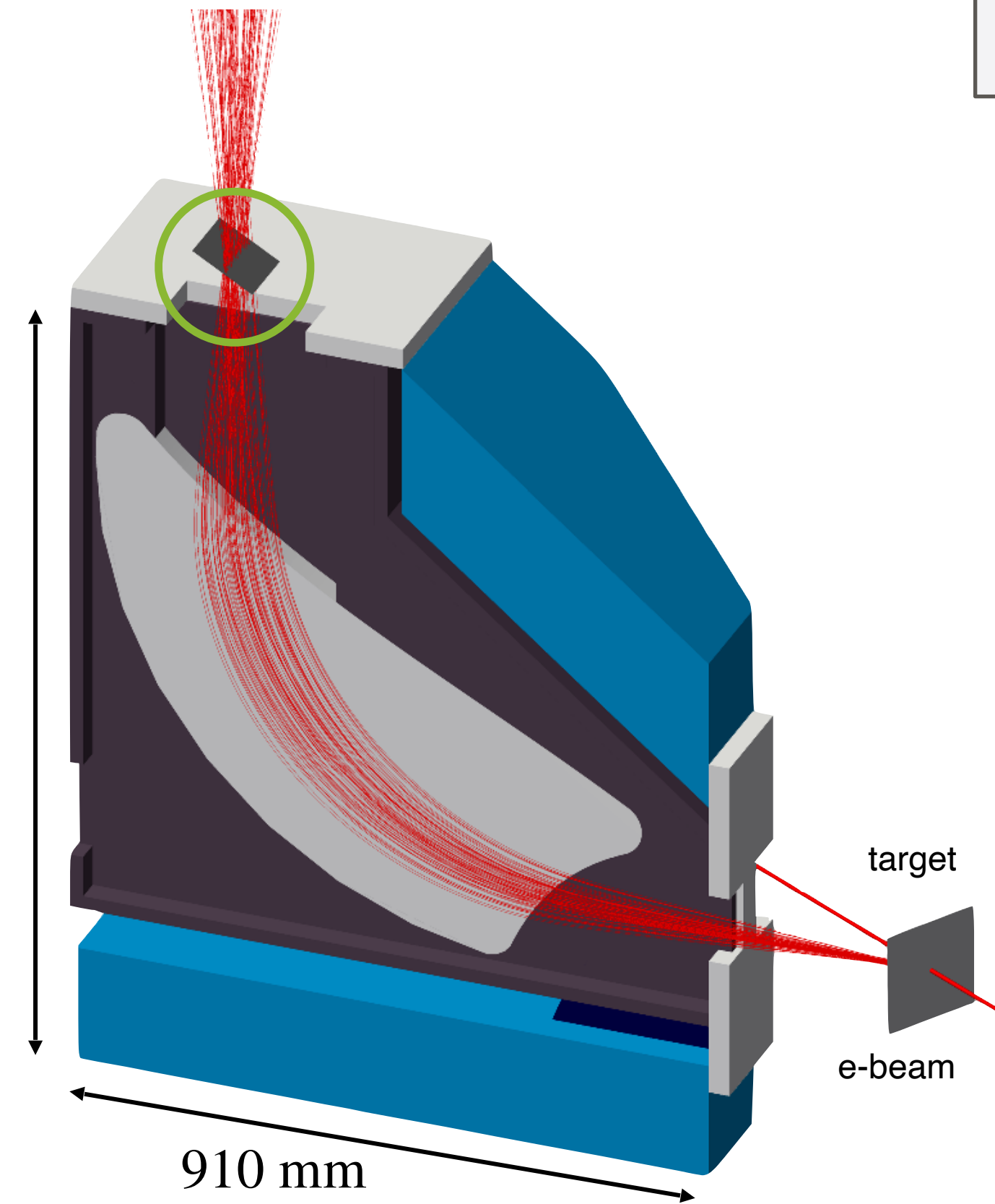
($\sim 1 \text{ mrad}$ accuracy)

$Q^2 = 3 \times 10^{-5} - 0.013 \text{ (GeV/c)}^2$

($\Delta Q^2/Q^2 \sim 10^{-3}$)

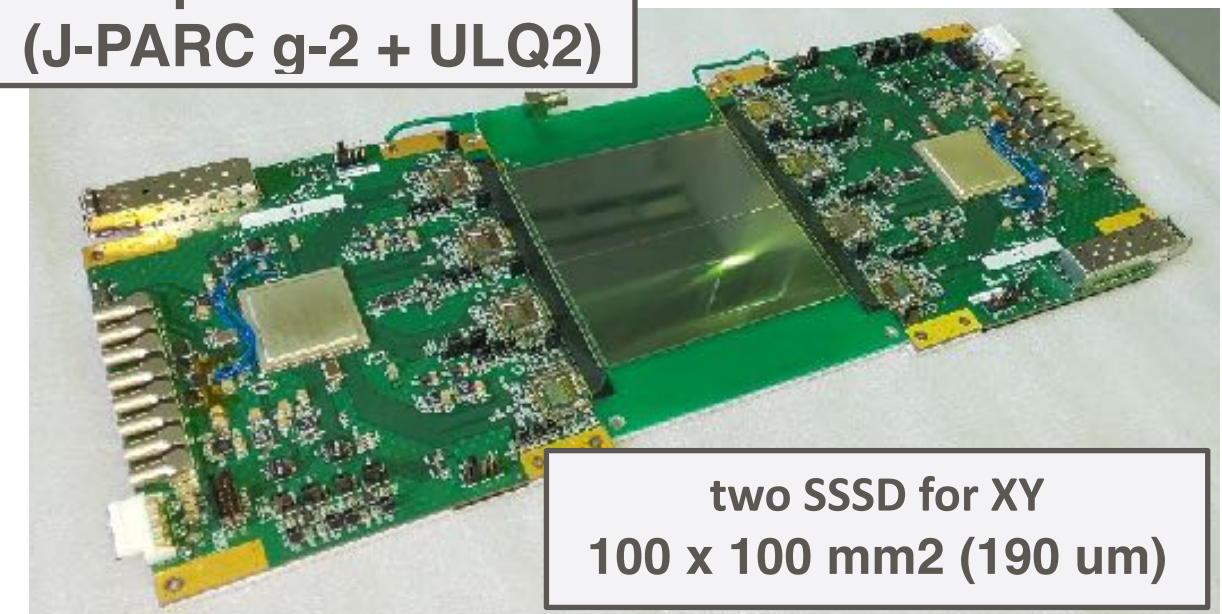


ULQ2 twin spectrometers



Y. Honda

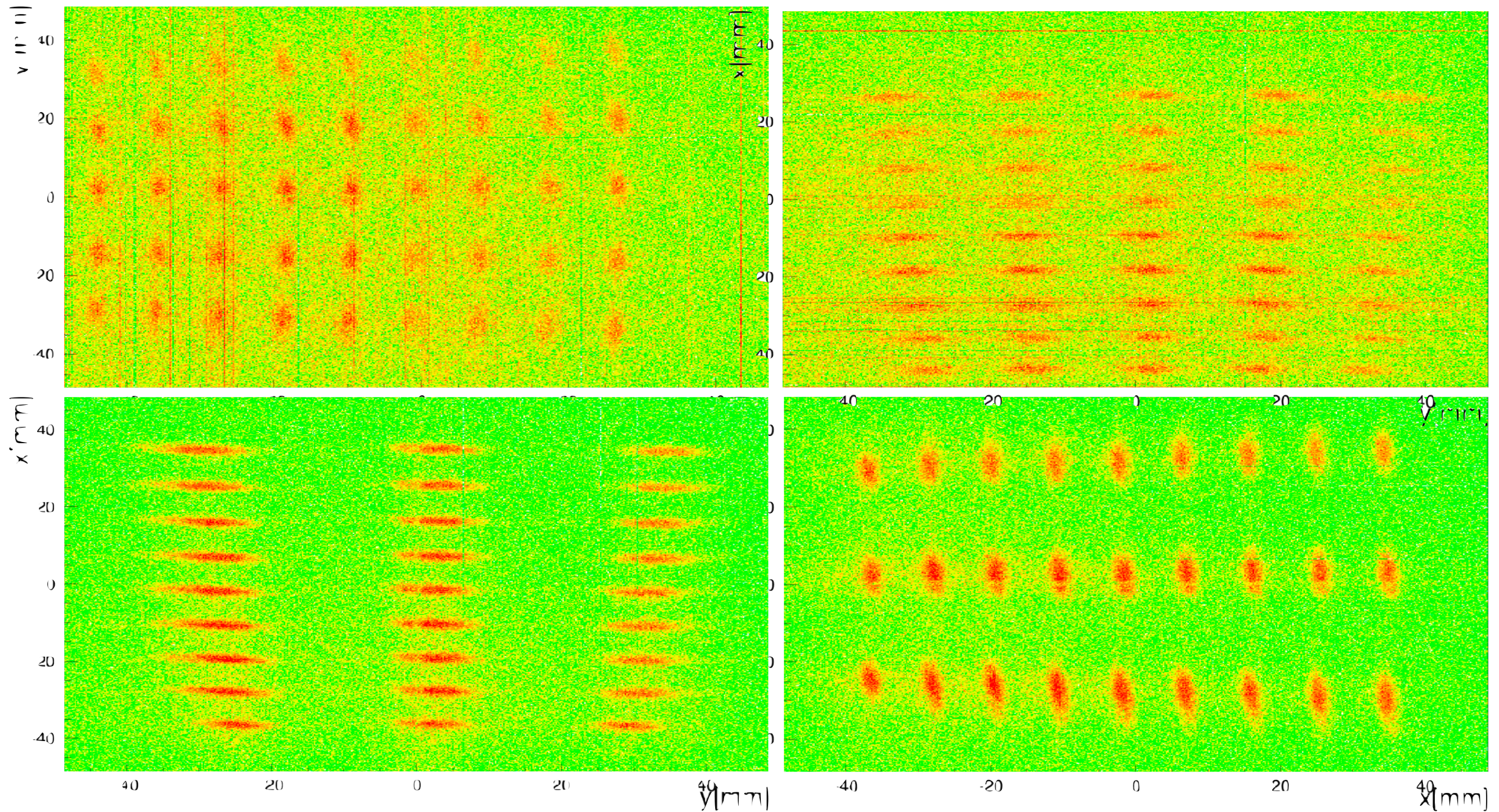
Focal plane detectors
(J-PARC g-2 + ULQ2)



two SSSD for XY
100 x 100 mm² (190 μm)

Electron spectrometer	
radius	500 mm
bending angle	90°
max. B	0.4T @ 60MeV
gap	70 mm
dispersion	866 mm
$\Delta p/p$	5.6×10^{-4}
momentum bite	10%
$\Delta\theta$	5 mrad
solid angle	6 mSr
weight	5 ton

ULQ2 spectrometer optics up to 2nd order



ULQ2 spectrometer optics up to 2nd order

Parameters	Spectrometer 1	Spectrometer 2
x_0 [mm]	4.9	-1.8
$(x_d \delta)$ [mm]	866.1(7)	862.4(7)
$(x_d^2 \delta)$ [mm]	-174(26)	-164(26)
$(x_d \Delta\theta^2)$ [10^{-4} mm/mrad 2]	-4.1(2)	-3.6(2)
θ_0 [mrad]	-2.9(5)	6.8(6)
$(y_d \Delta\theta)$ [mm/mrad]	0.999(4)	0.997(3)
$(y_d \delta\Delta\theta)$ [mm/mrad]	2.01(14)	1.92(11)
$(x_d x_b), (y_d y_b)$ [mm/mm]	$\sim 0.5, 1.8$	

ULQ2 Physics Program

1) Proton : charge radius

$\text{CH}_2(e,e')$

aiming at the “least model-dependent” $G_E(Q^2)$ determination

under **lowest-ever Q^2**

absolute cross section measurement

Rosenbluth separated $G_E(Q^2)$ and $G_M(Q^2)$ *if necessary*

2) Deuteron : charge radius

$\text{CD}_2(e,e')$

possible determination of neutron charge radius

3) ^{208}Pb elastic scattering

$^{208}\text{Pb}(e,e')$

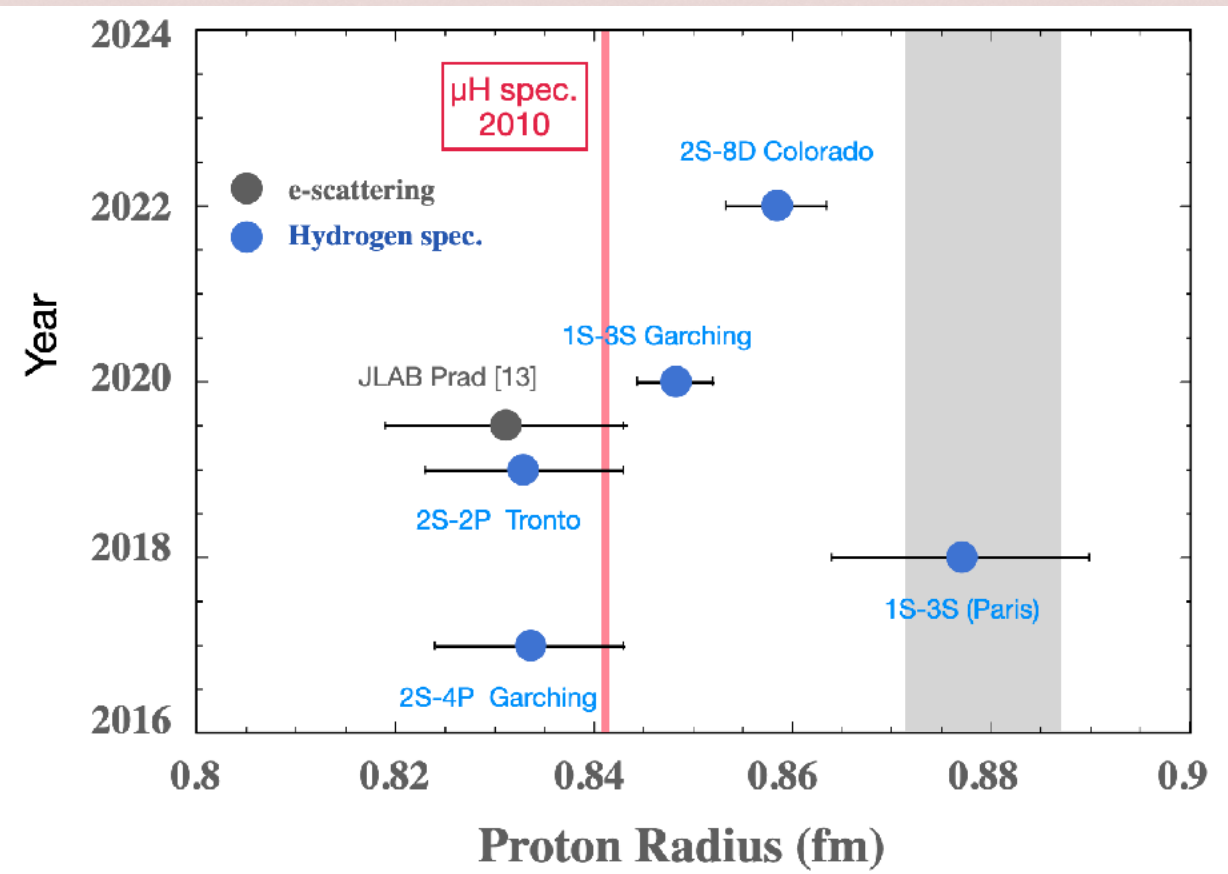
4th moment of charge density distribution

=> neutron-distribution radius

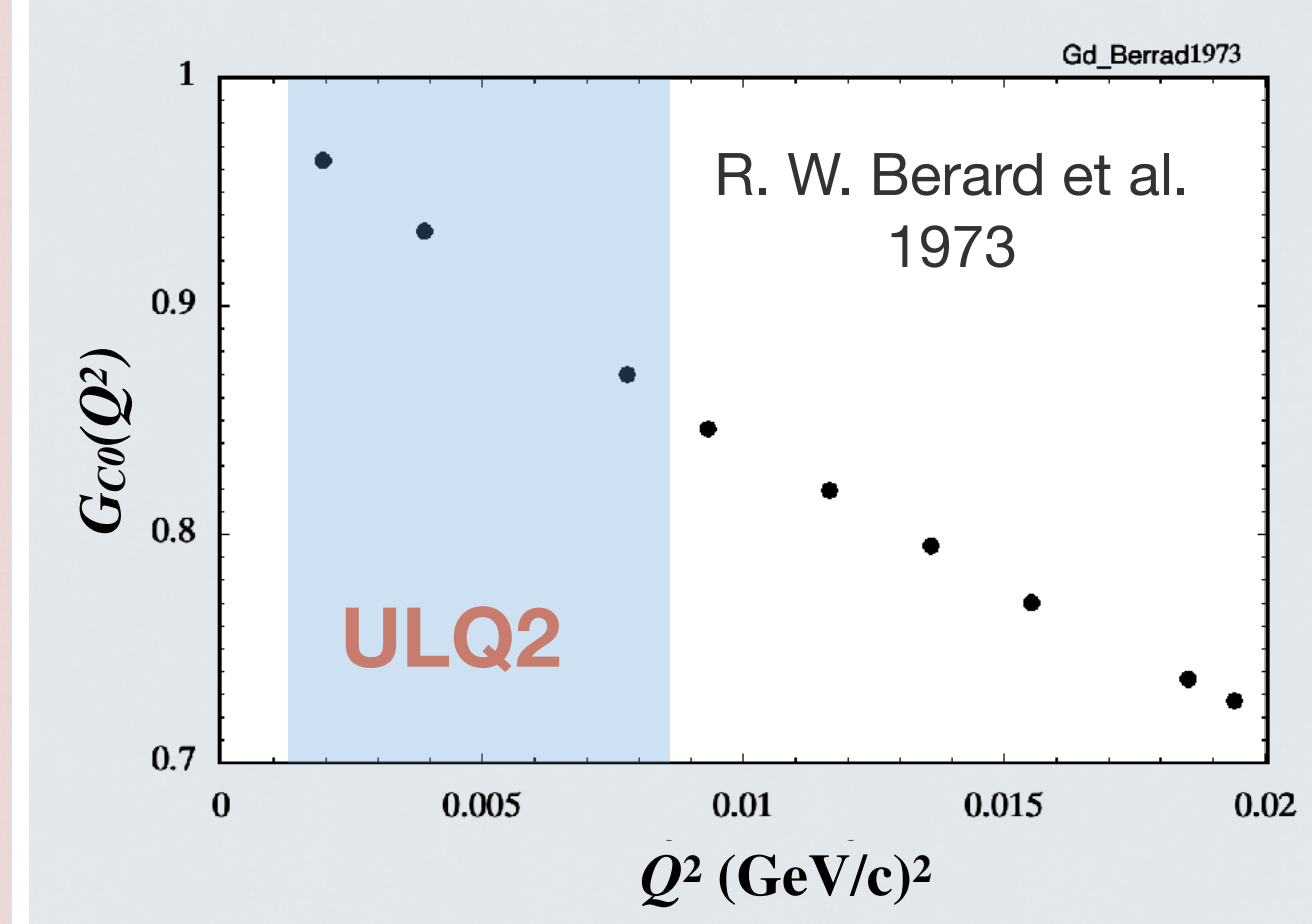
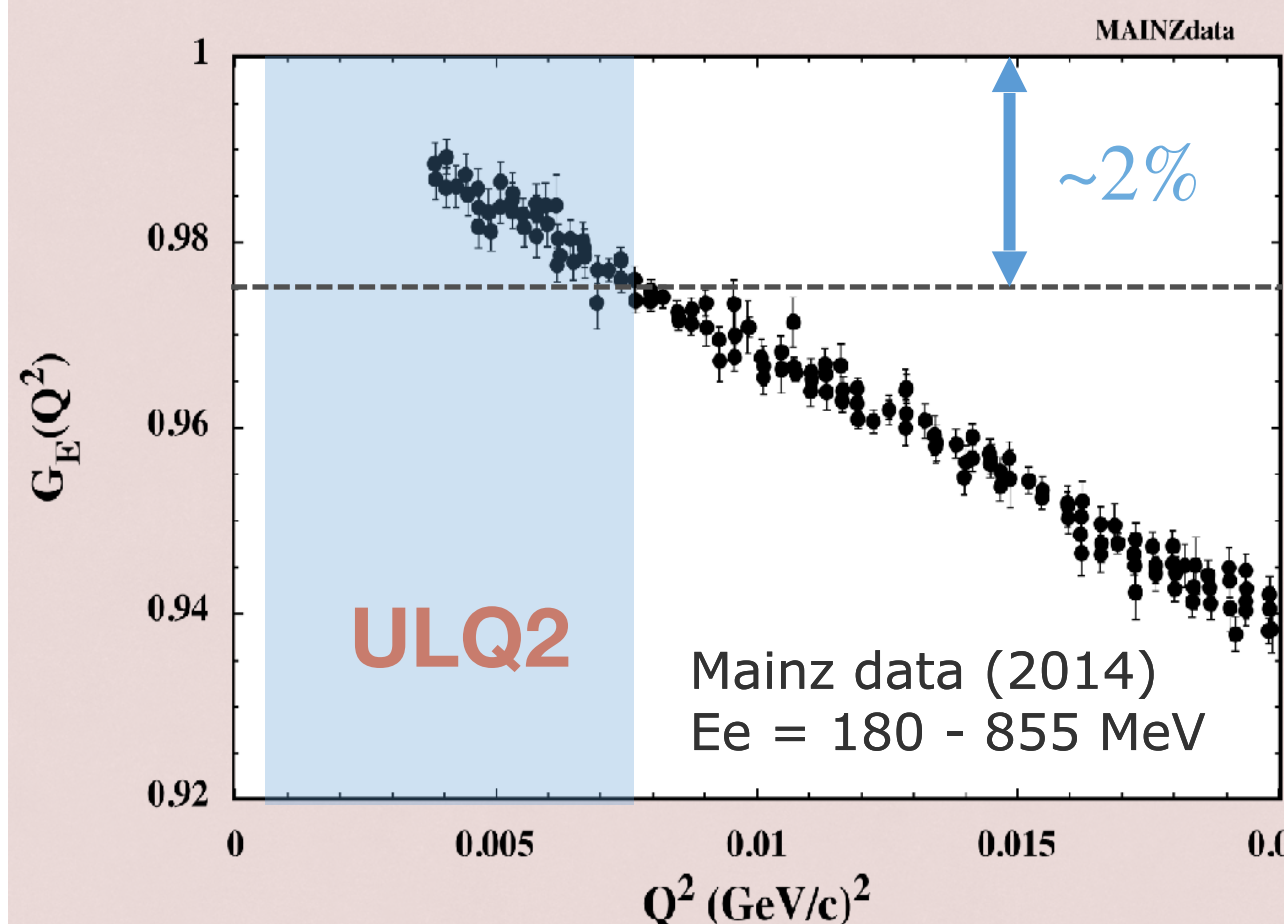
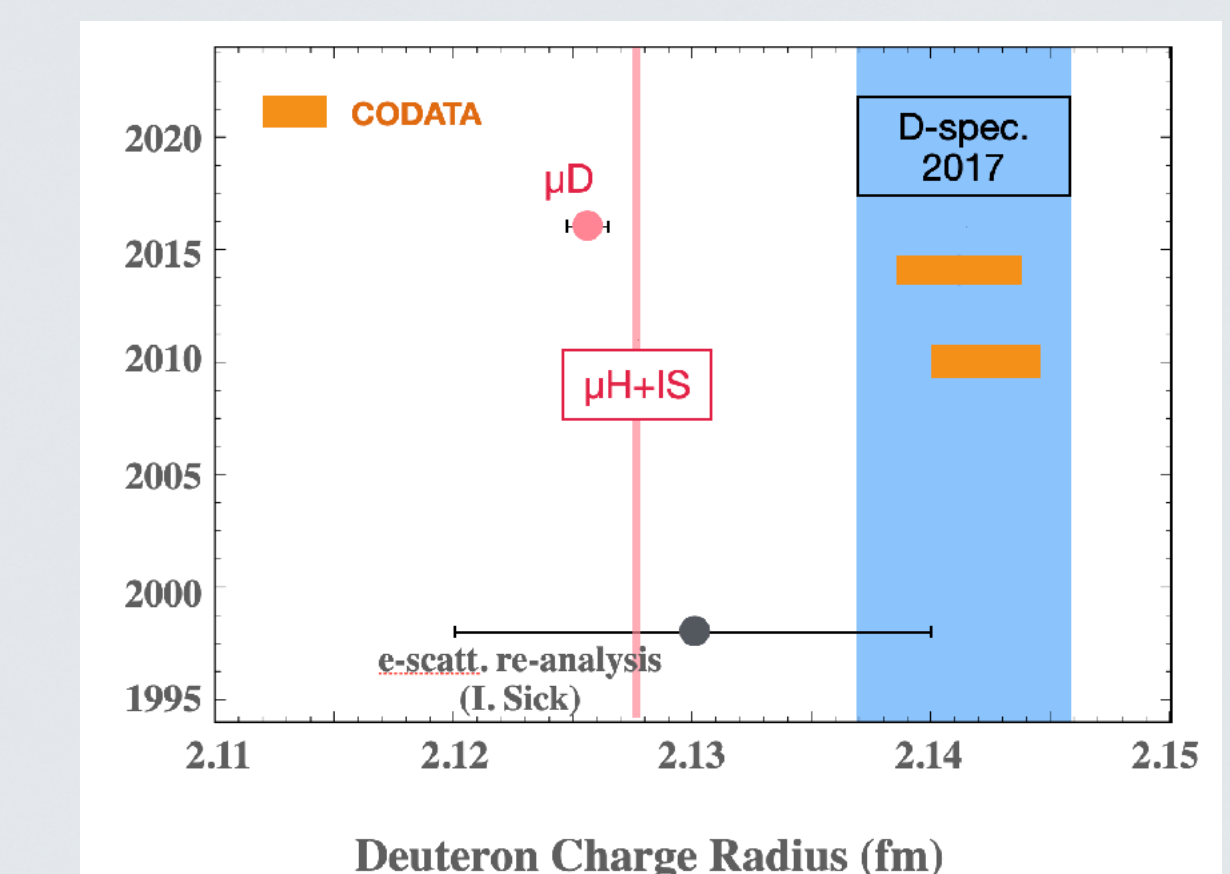
cross section under never-yet-measured low- q region

$q = 5 - 100 \text{ MeV}$

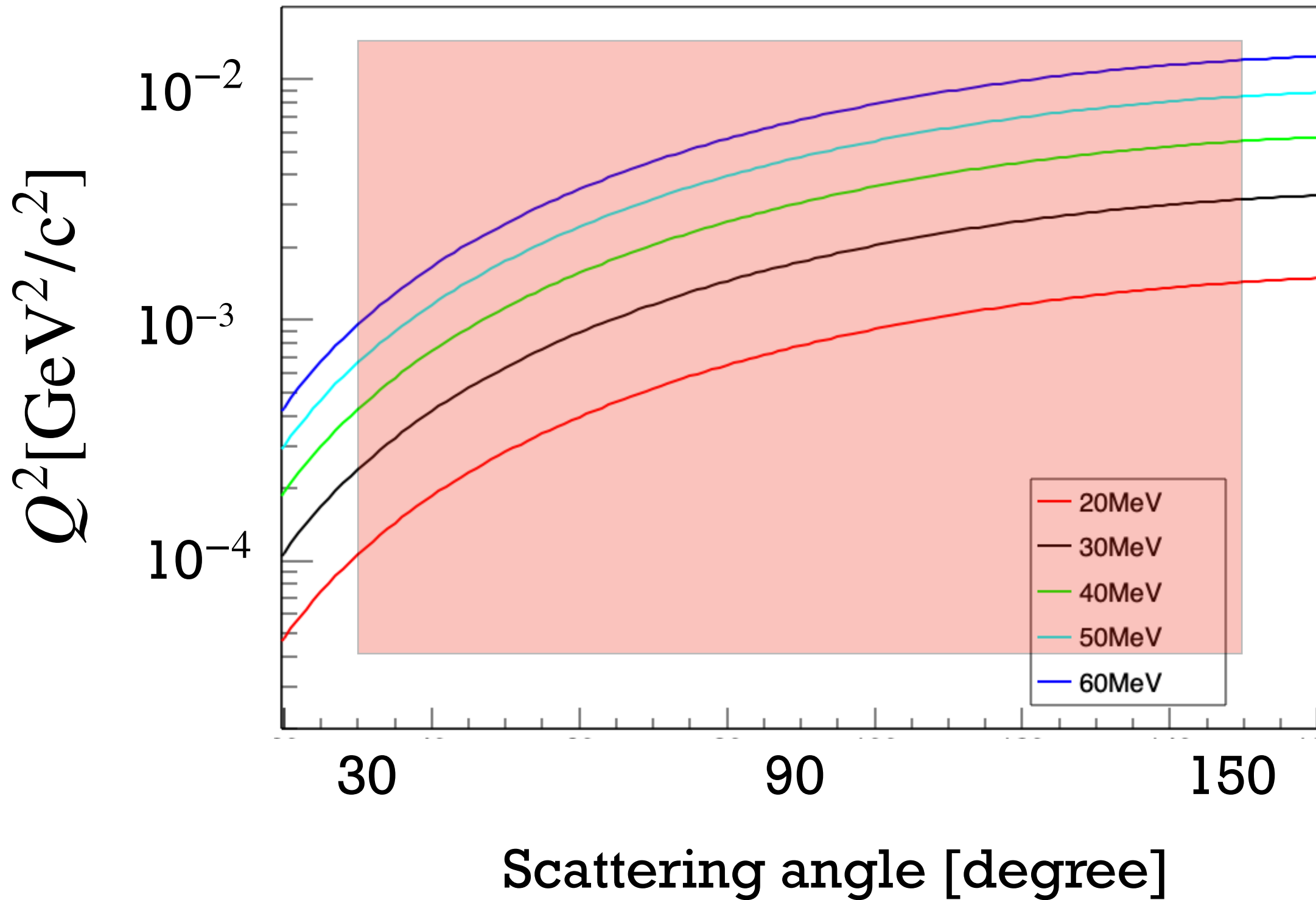
proton



deuteron



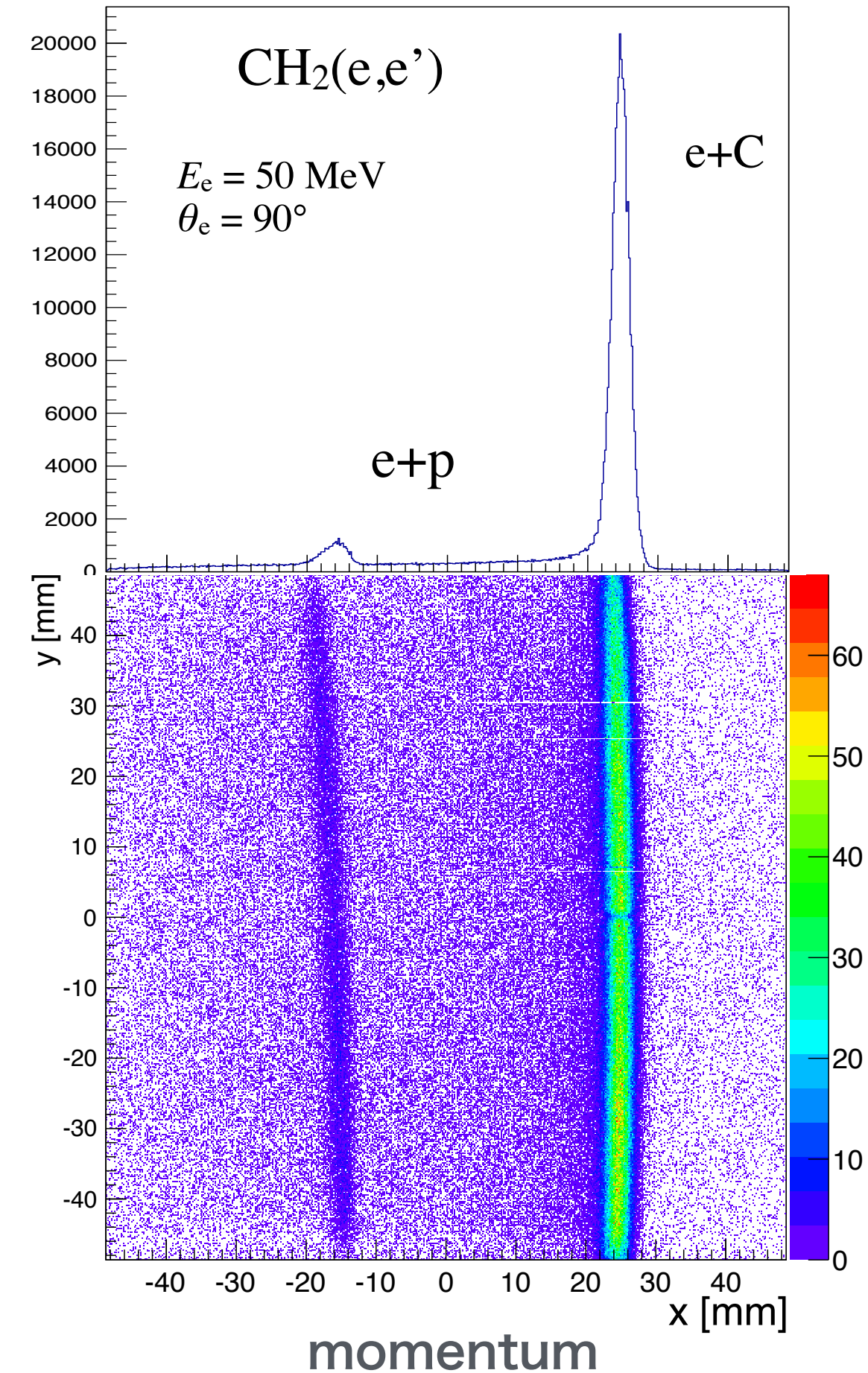
ULQ2 kinematics



Absolute cross section

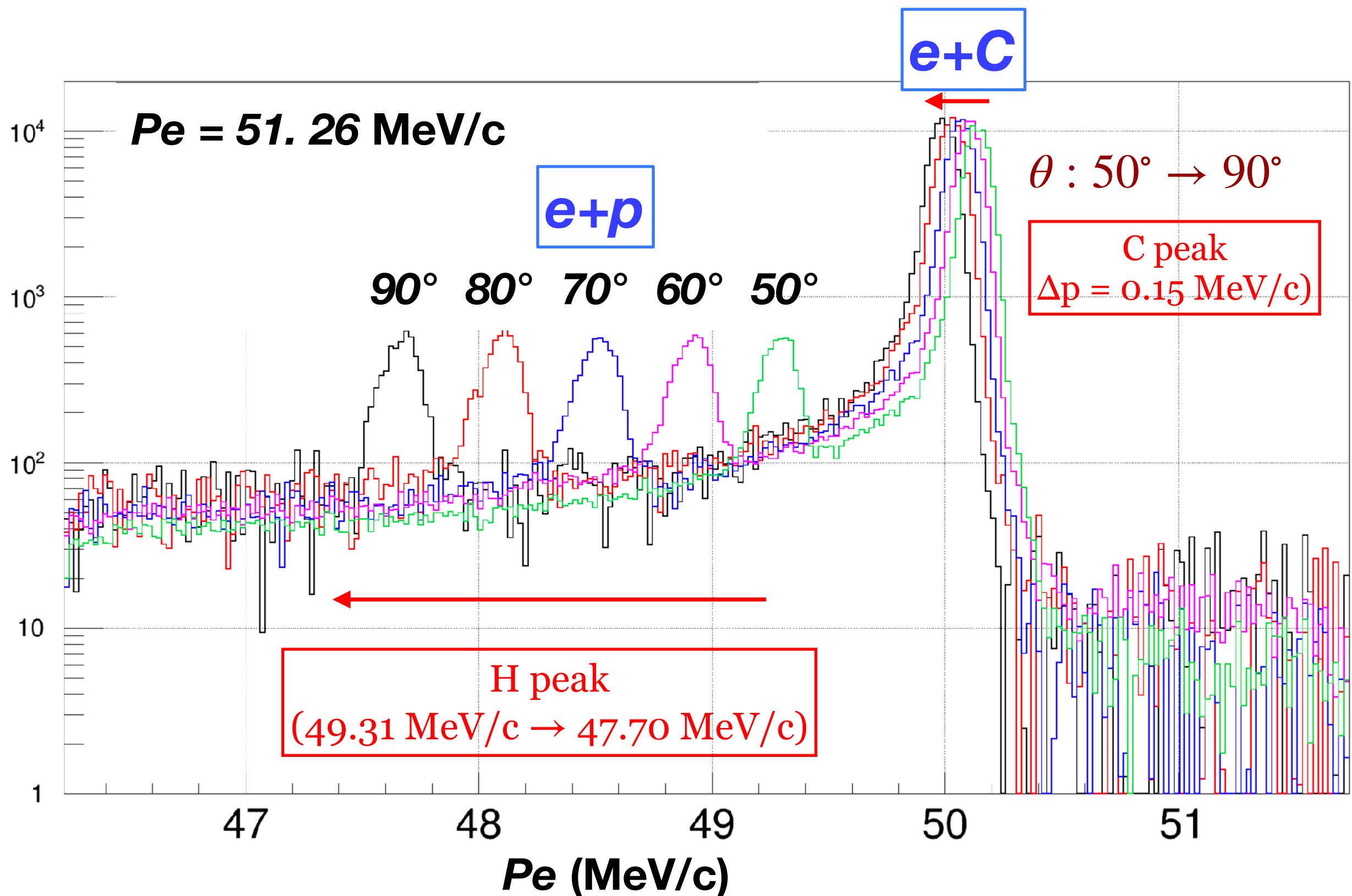
CH_2 (CD_2) as targets

- 1) thin solid target ($\sim 100 \text{ }\mu\text{m}$)
- 2) simultaneous detection
of $e+C$ and $e+p$ (d) scattering
- 3) $\langle r_c^2 \rangle$ of ^{12}C : accuracy $\sim 10^{-3}$
- 4) $\Delta Q^2/Q^2 \leq 10^{-3}$

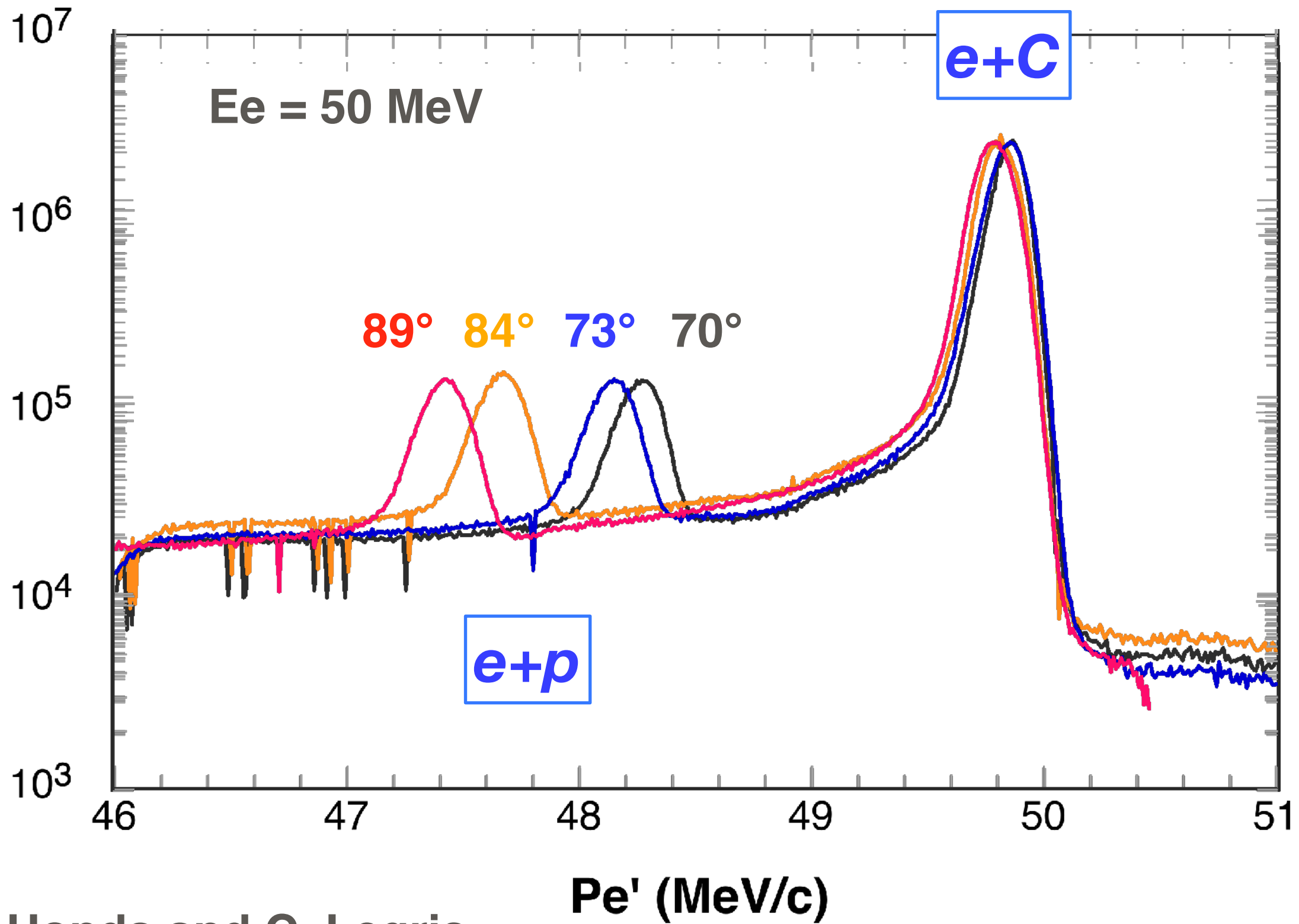


CH₂ target

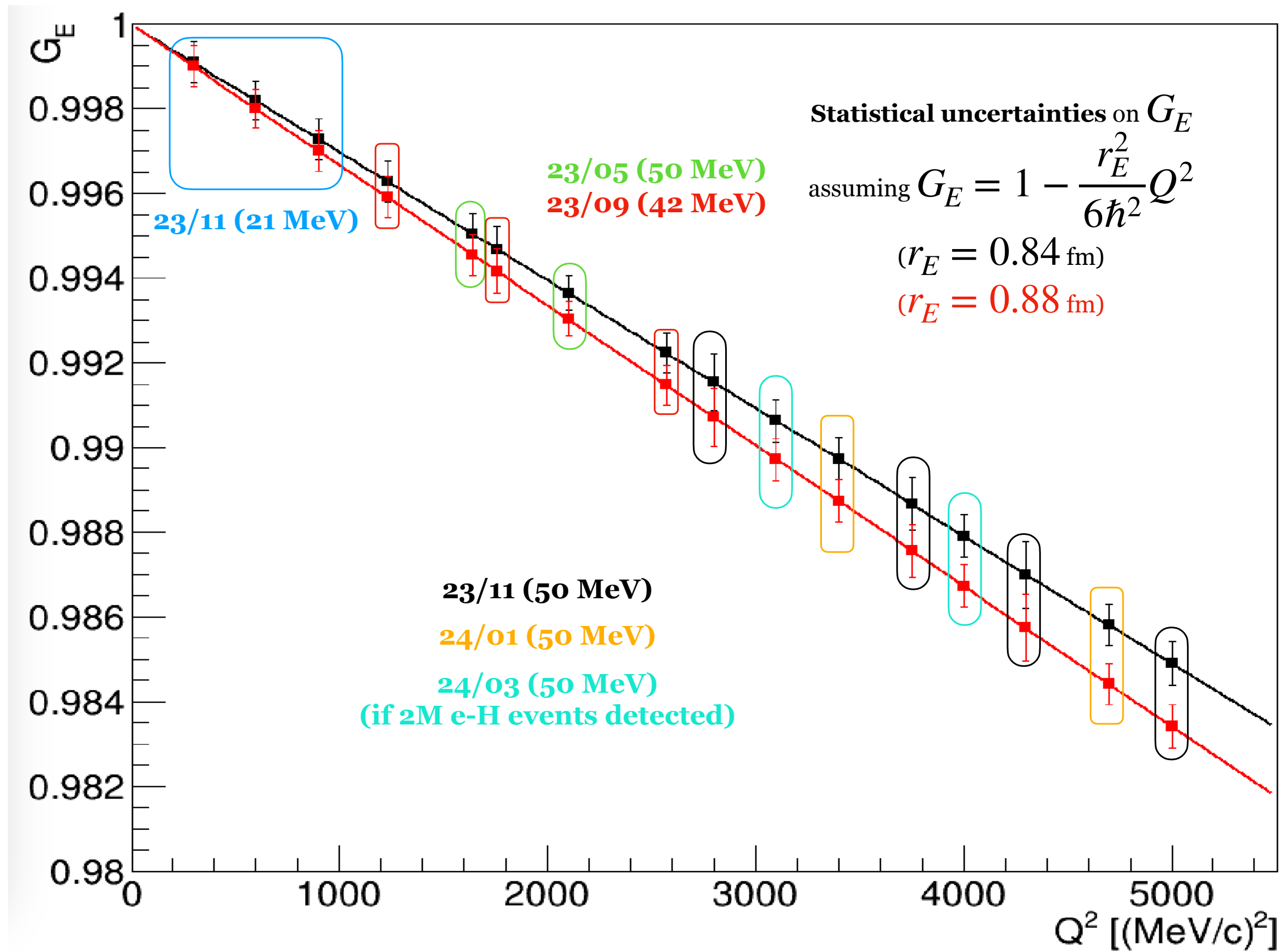
relative measurement to well-known e+¹²C scattering

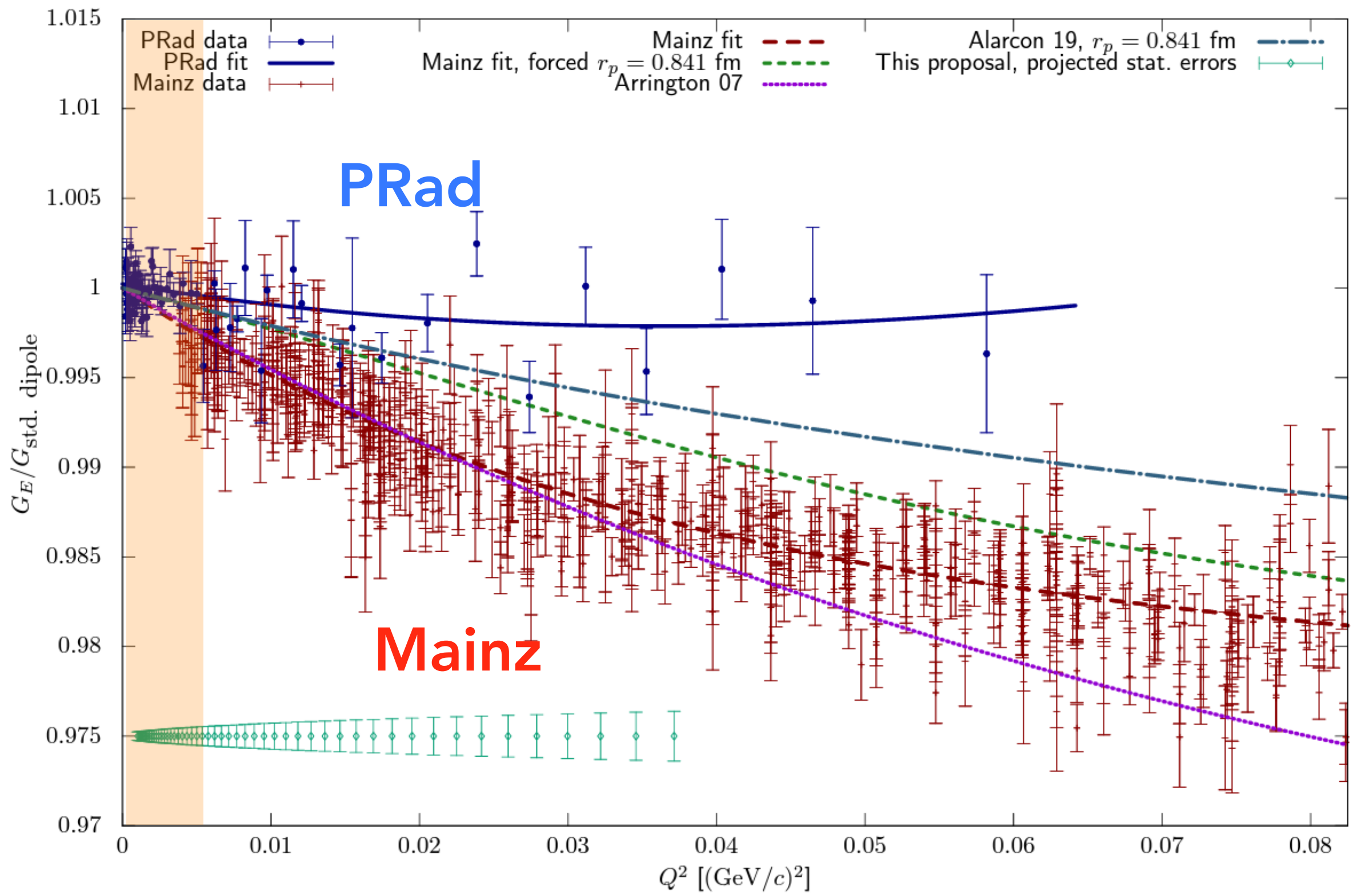


typical spectra of CH₂(e,e') @ ULQ2



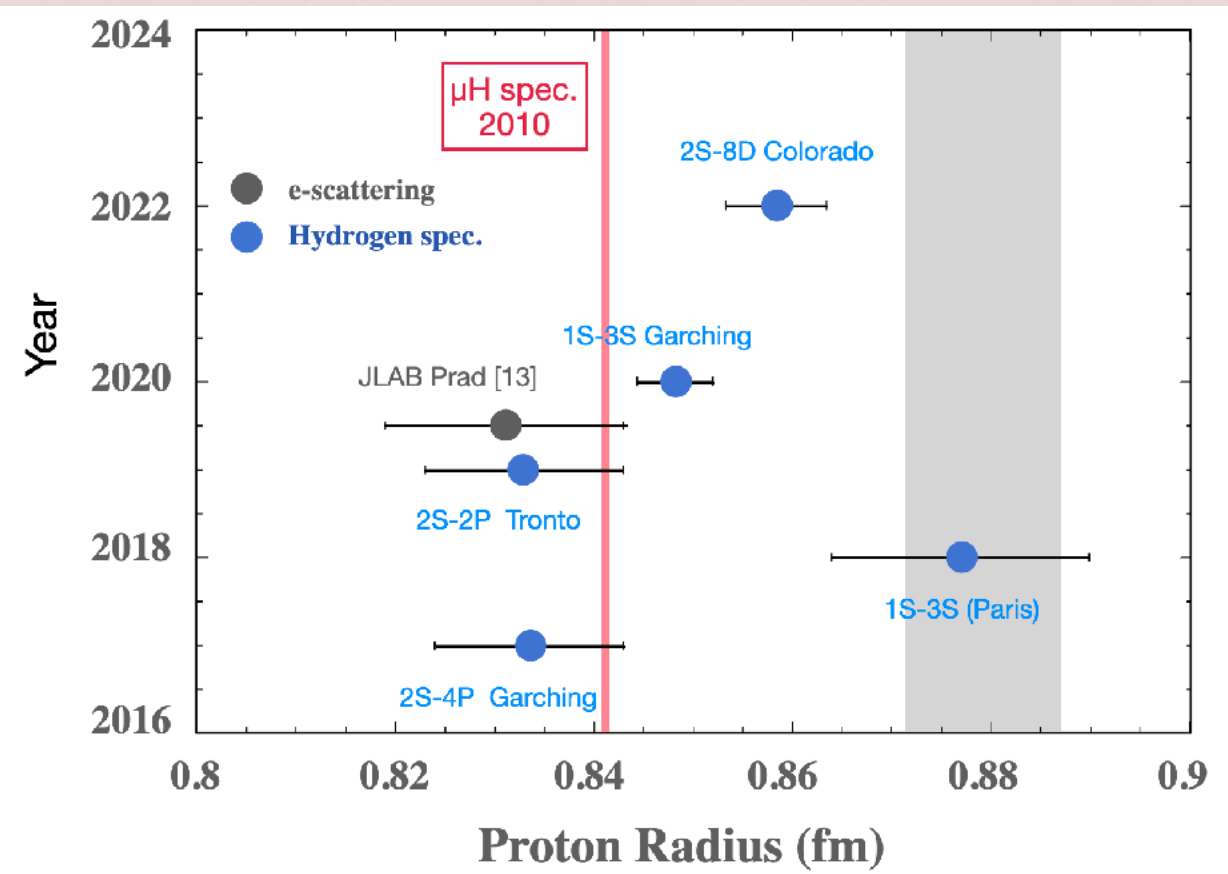
Q^2 : 14 measured/ 16 planned



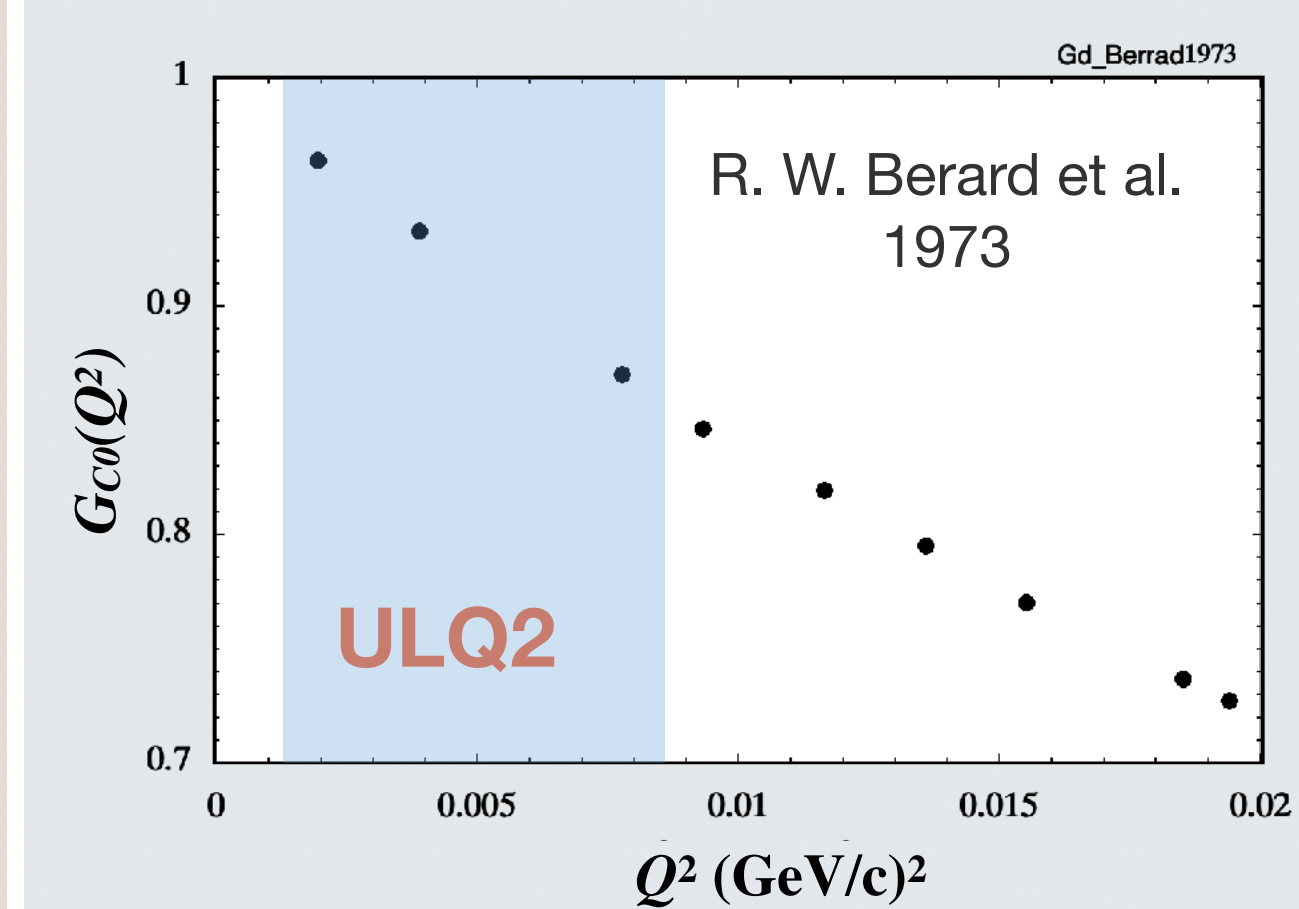
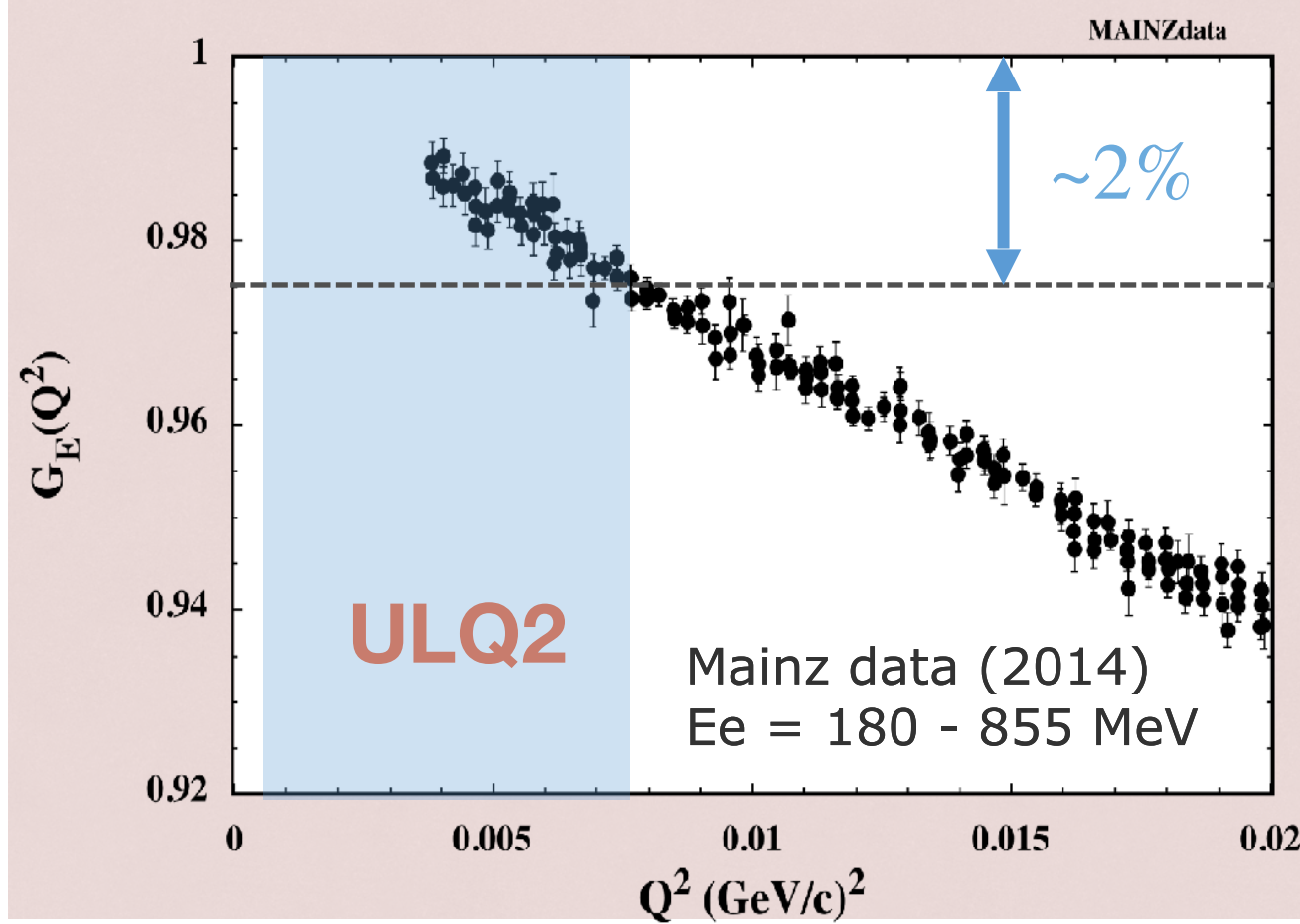
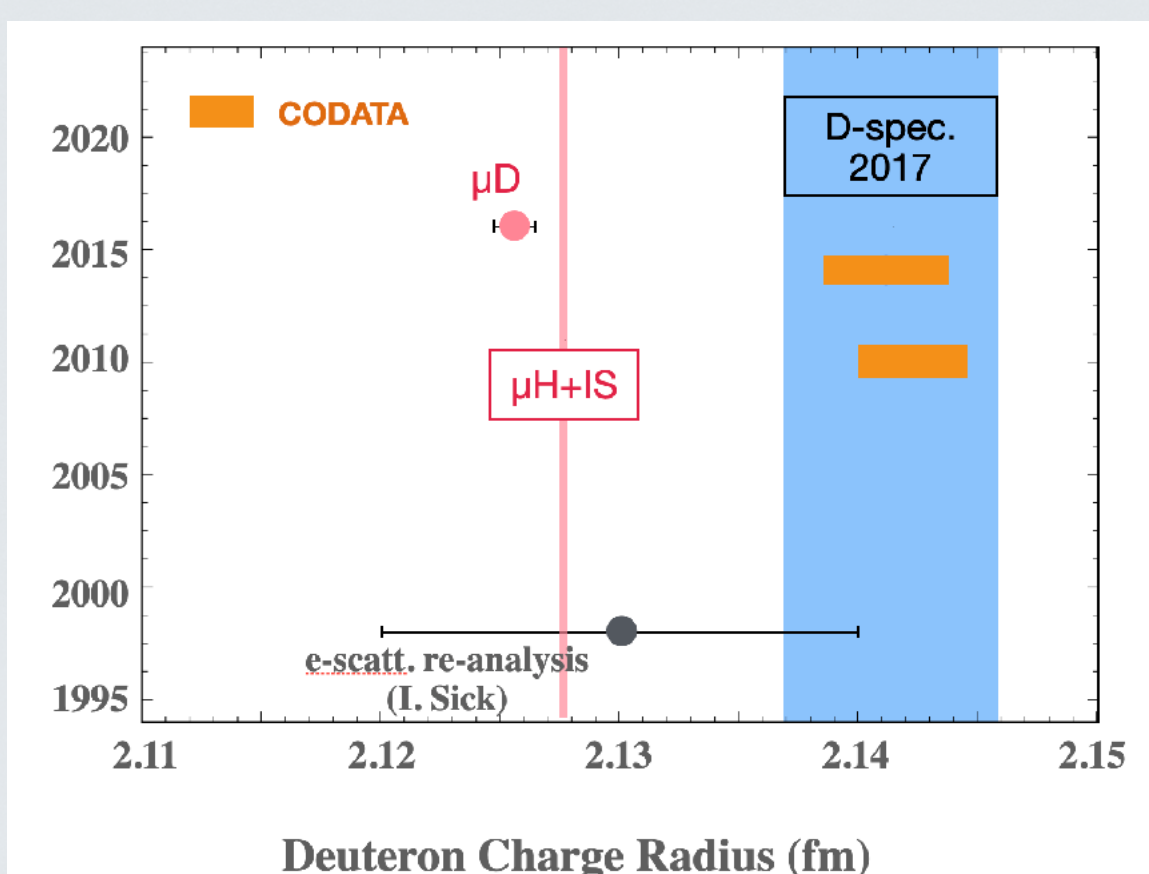


**additional physics opportunity
at ULQ2**

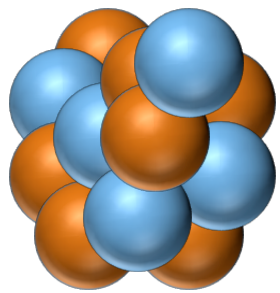
proton



deuteron



nuclear charge density, moments



Proton

Neutron

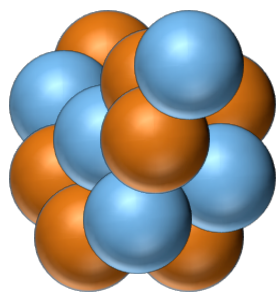
1) charge density

$$\rho_c(r) = \rho_c^p(r) + \rho_c^n(r)$$

$$\rho_c^p(r) = \int \rho_p(r) \rho_{p(point)}(r - r') d^3r'$$

$$\rho_c^n(r) = \int \rho_n(r) \rho_{n(point)}(r - r') d^3r'$$

nuclear charge density, moments



Proton

Neutron

1) charge density

$$\rho_c(r) = \rho_c^p(r) + \rho_c^n(r)$$

$$\rho_c^p(r) = \int \rho_p(r) \rho_{p(point)}(r - r') d^3r'$$

$$\rho_c^n(r) = \int \rho_n(r) \rho_{n(point)}(r - r') d^3r'$$

2) 2nd moment

$$\langle r_c^2 \rangle = \int r^2 \rho_c(r) d^3r \quad \text{Proton}$$

$$= \langle r_{p(point)}^2 \rangle + \langle r_p^2 \rangle +$$

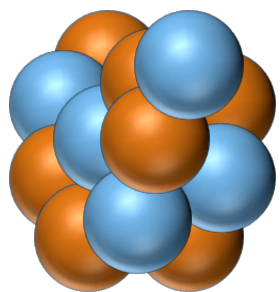


Neutron



$$\langle r_{n(point)}^2 \rangle + \frac{N}{Z} \langle r_n^2 \rangle + \text{rel. corr.}$$

nuclear charge density, moments



Proton

Neutron

1) charge density

$$\rho_c(r) = \rho_c^p(r) + \rho_c^n(r)$$

$$\rho_c^p(r) = \int \rho_p(r) \rho_{p(point)}(r - r') d^3r'$$

$$\rho_c^n(r) = \int \rho_n(r) \rho_{n(point)}(r - r') d^3r'$$

2) 2nd moment

$$\langle r_c^2 \rangle = \int r^2 \rho_c(r) d^3r \quad \text{Proton}$$

$$= \langle r_{p(point)}^2 \rangle + \langle r_p^2 \rangle +$$

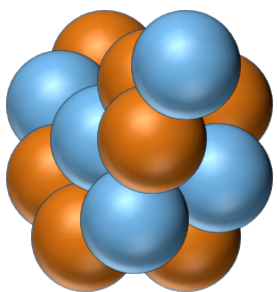


Neutron



$$\cancel{\langle r_{n(point)}^2 \rangle} + \frac{N}{Z} \langle r_n^2 \rangle + \text{rel. corr.}$$

nuclear charge density, moments



Proton

Neutron

1) charge density

$$\rho_c(r) = \rho_c^p(r) + \rho_c^n(r)$$

$$\rho_c^p(r) = \int \rho_p(r) \rho_{p(point)}(r - r') d^3r'$$

$$\rho_c^n(r) = \int \rho_n(r) \rho_{n(point)}(r - r') d^3r'$$

2) 2nd moment exp.

$$\langle r_c^2 \rangle = \int r^2 \rho_c(r) d^3r \quad \text{Proton}$$

$$= \langle r_{p(point)}^2 \rangle + \langle r_p^2 \rangle +$$

$$\cancel{\langle r_{n(point)}^2 \rangle} + \frac{N}{Z} \langle r_n^2 \rangle + \text{rel. corr.}$$

theories

3) 4th moment

$$\langle r_c^4 \rangle = \int r^4 \rho_c(r) d^3r$$

3) 4th moment

$$\langle r_c^4 \rangle = \int r^4 \rho_c(r) d^3r$$

$$= \langle r_{p(point)}^4 \rangle + \frac{10}{3} \langle r_{p(point)}^2 \rangle \langle r_p^2 \rangle$$

$$+ \langle r_{n(point)}^4 \rangle + \frac{10}{3} \langle r_{n(point)}^2 \rangle \langle r_n^2 \rangle \frac{N}{Z}$$

+ rel. corr.

3) 4th moment

$$\langle r_c^4 \rangle = \int r^4 \rho_c(r) d^3r$$

$$= \langle r_{p(point)}^4 \rangle + \frac{10}{3} \langle r_{p(point)}^2 \rangle \langle r_p^2 \rangle$$

$$+ \langle r_{n(point)}^4 \rangle + \frac{10}{3} \langle r_{n(point)}^2 \rangle \langle r_n^2 \rangle \frac{N}{Z}$$

+ rel. corr.

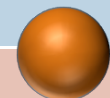
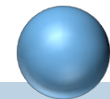
3) 4th moment

$$\langle r_c^4 \rangle = \int r^4 \rho_c(r) d^3r$$

$$= \langle r_{p(point)}^4 \rangle + \frac{10}{3} \langle r_{p(point)}^2 \rangle \langle r_p^2 \rangle$$

$$+ \cancel{\langle r_{p(point)}^4 \rangle} + \frac{10}{3} \langle r_{n(point)}^2 \rangle \langle r_n^2 \rangle \frac{N}{Z}$$

+ rel. corr.

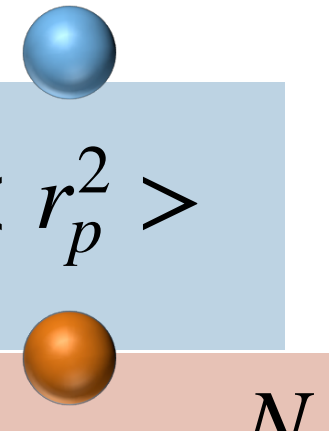


3) 4th moment

$$\langle r_c^4 \rangle = \int r^4 \rho_c(r) d^3r$$

$$\begin{aligned} &= \langle r_{p(point)}^4 \rangle + \frac{10}{3} \langle r_{p(point)}^2 \rangle \langle r_p^2 \rangle \\ &+ \cancel{\langle r_{p(point)}^4 \rangle} + \frac{10}{3} \cancel{\langle r_{n(point)}^2 \rangle} \langle r_n^2 \rangle \frac{N}{Z} \end{aligned}$$

+ rel. corr.
RMS n-radius



3) 4th moment

$$\langle r_c^4 \rangle = \int r^4 \rho_c(r) d^3r$$

exp.

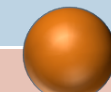
theories

$$= \langle r_{p(point)}^4 \rangle + \frac{10}{3} \langle r_{p(point)}^2 \rangle \langle r_p^2 \rangle$$

$$+ \cancel{\langle r_{p(point)}^4 \rangle} + \frac{10}{3} \cancel{\langle r_{n(point)}^2 \rangle} \langle r_n^2 \rangle \frac{N}{Z}$$

+ rel. corr .

RMS n-radius



- 1) H. Kurasawa and T. Suzuki, Prog. Theor. Exp. Phys. 2019, 113D01
- 2) H. Kurasawa, T. S. and T. Suzuki, Prog. Theor. Exp. Phys. 2021, 013D02
- 3) H. Kurasawa and T. Suzuki, Prog. Theor. Exp. Phys. 2022, 023D03
- 4) T. Suzuki, Prog. Theor. Exp. Phys. submitted

deuteron

2nd moment

$$\langle r_c^2 \rangle = \boxed{\langle r_{p(point)}^2 \rangle} + \langle r_p^2 \rangle + \langle r_n^2 \rangle + \text{rel. corr.}$$

isotope shift measurement

$$\langle r_c^2 \rangle - \langle r_p^2 \rangle = 3.82070(31) \text{ fm}^2$$

deuteron

2nd moment

$$\langle r_c^2 \rangle = \boxed{\langle r_{p(point)}^2 \rangle} + \langle r_p^2 \rangle + \langle r_n^2 \rangle + \text{rel. corr.}$$

isotope shift measurement

$$\langle r_c^2 \rangle - \langle r_p^2 \rangle = 3.82070(31) \text{ fm}^2$$

4th moment

$$\begin{aligned} \langle r_c^4 \rangle &= \langle r_{p(point)}^4 \rangle + \frac{10}{3} \langle r_{p(point)}^2 \rangle \langle r_p^2 \rangle \\ &\quad + \frac{10}{3} \langle r_{n(point)}^2 \rangle \langle r_n^2 \rangle + \text{rel. corr.} \end{aligned}$$

deuteron

2nd moment

$$\langle r_c^2 \rangle = \boxed{\langle r_{p(point)}^2 \rangle} + \langle r_p^2 \rangle + \langle r_n^2 \rangle + \text{rel. corr.}$$

isotope shift measurement

$$\langle r_c^2 \rangle - \langle r_p^2 \rangle = 3.82070(31) \text{ fm}^2$$

4th moment

$$\langle r_c^4 \rangle = \langle r_{p(point)}^4 \rangle + \frac{10}{3} \langle r_{p(point)}^2 \rangle \langle r_p^2 \rangle$$

$$r_{p(point)} \quad r_{n(point)} \quad + \frac{10}{3} \langle r_{n(point)}^2 \rangle \langle r_n^2 \rangle + \text{rel. corr.}$$



deuteron

2nd moment

$$\langle r_c^2 \rangle = \boxed{\langle r_{p(\text{point})}^2 \rangle} + \langle r_p^2 \rangle + \langle r_n^2 \rangle + \text{rel. corr.}$$

isotope shift measurement

$$\langle r_c^2 \rangle - \langle r_p^2 \rangle = 3.82070(31) \text{ fm}^2$$

4th moment

$$\langle r_c^4 \rangle = \langle r_{p(\text{point})}^4 \rangle + \frac{10}{3} \langle r_{p(\text{point})}^2 \rangle \langle r_p^2 \rangle$$

$$r_{p(\text{point})} \quad r_{n(\text{point})} \quad + \frac{10}{3} \langle r_{n(\text{point})}^2 \rangle \langle r_n^2 \rangle + \text{rel. corr.}$$



$$= \boxed{\langle r_{p(\text{point})}^4 \rangle} + \frac{10}{3} \boxed{\langle r_{p(\text{point})}^2 \rangle} (\langle r_p^2 \rangle + \langle r_n^2 \rangle) + \text{rel. corr.}$$

Extraction of the Neutron Charge Radius from a Precision Calculation of the Deuteron Structure Radius

A. A. Filin¹, V. Baru^{2,3,4}, E. Epelbaum¹, H. Krebs¹, D. Möller¹, and P. Reinert¹

¹*Ruhr-Universität Bochum, Fakultät für Physik und Astronomie, Institut für Theoretische Physik II,
D-44780 Bochum, Germany*

²*Helmholtz-Institut für Strahlen- und Kernphysik and Bethe Center for Theoretical Physics, Universität Bonn,
D-53115 Bonn, Germany*

³*Institute for Theoretical and Experimental Physics NRC “Kurchatov Institute”, Moscow 117218, Russia*

⁴*P.N. Lebedev Physical Institute of the Russian Academy of Sciences, 119991, Leninskiy Prospect 53, Moscow, Russia*

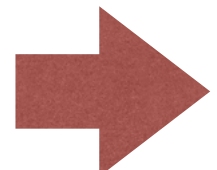
$$\begin{array}{ccc}
 < r_c^2 > = < r_{str}^2 > + < r_p^2 > + < r_n^2 > + \text{rel. corr.} \\
 \mu\text{D spec.} \quad \chi\text{EFT}
 \end{array}$$

$$< r_{str}^2 > = (1.9731 {}^{+0.0013}_{-0.0018})^2 \text{ fm}^2$$

$$< r_c^2 > = (2.12560(78))^2 \text{ fm}^2$$

$$< r_p^2 > = (0.8414(9))^2 \text{ fm}^2$$

$$\text{rel. corr. : } - \frac{3}{4m^2} \quad (\text{Darwin-Foldy})$$

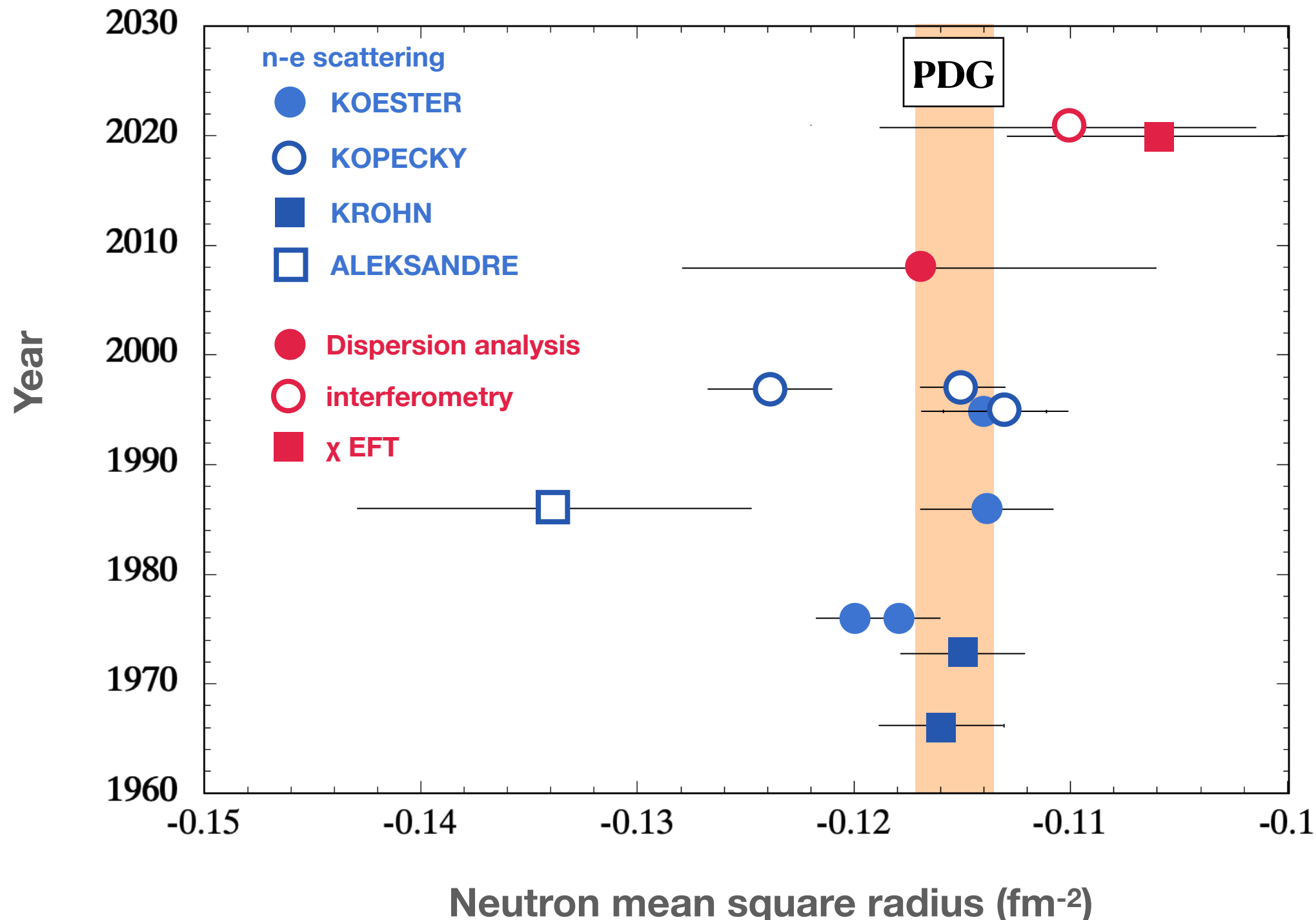


$$< r_n^2 > = -0.106 {}^{+0.007}_{-0.005} \text{ fm}^2$$

neutron charge radius original figure

PDG $\langle r_{n2} \rangle = -0.1155 \pm 0.0017 \text{ fm}^2$

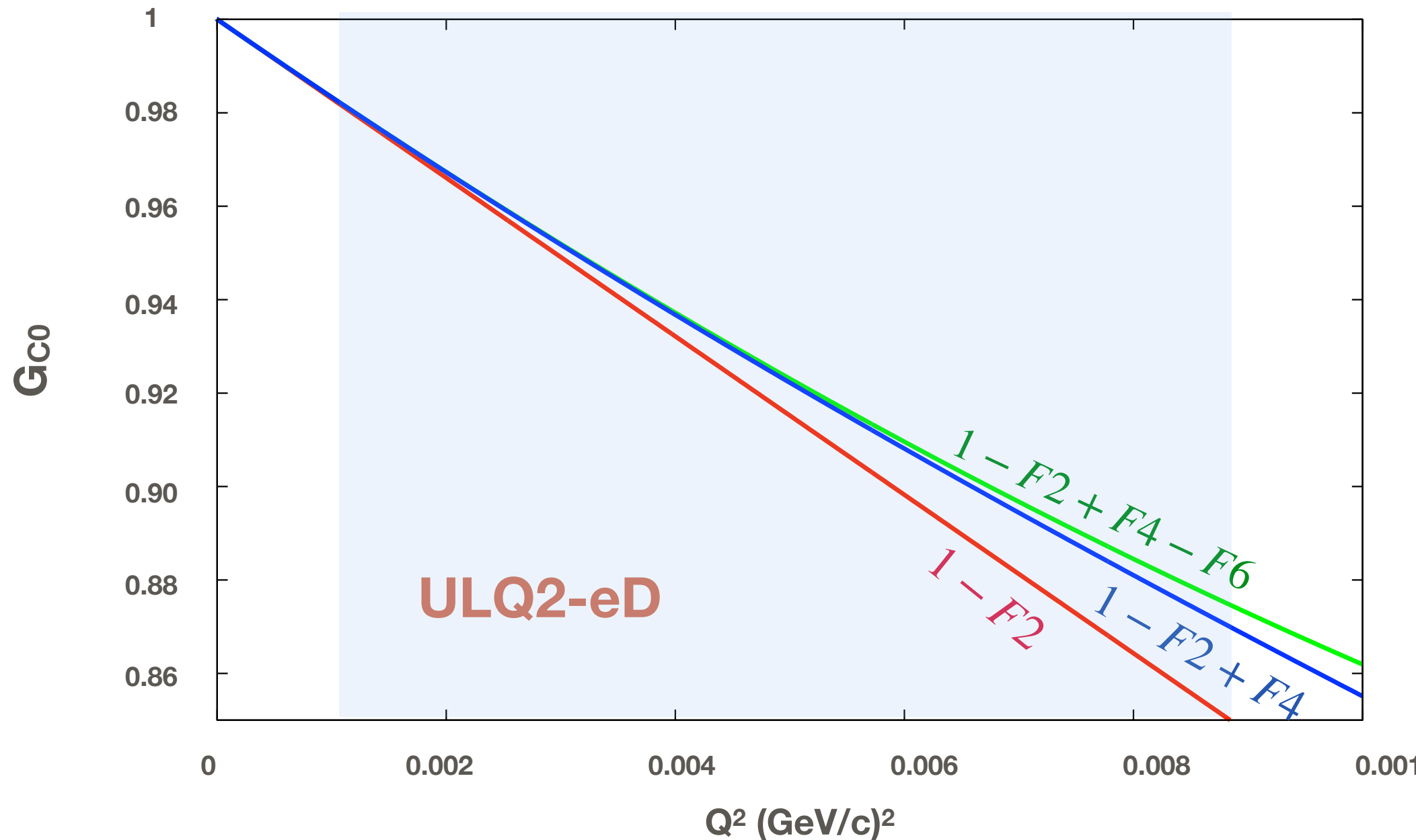
中性子半径グラフ2023_KG_枠のみ



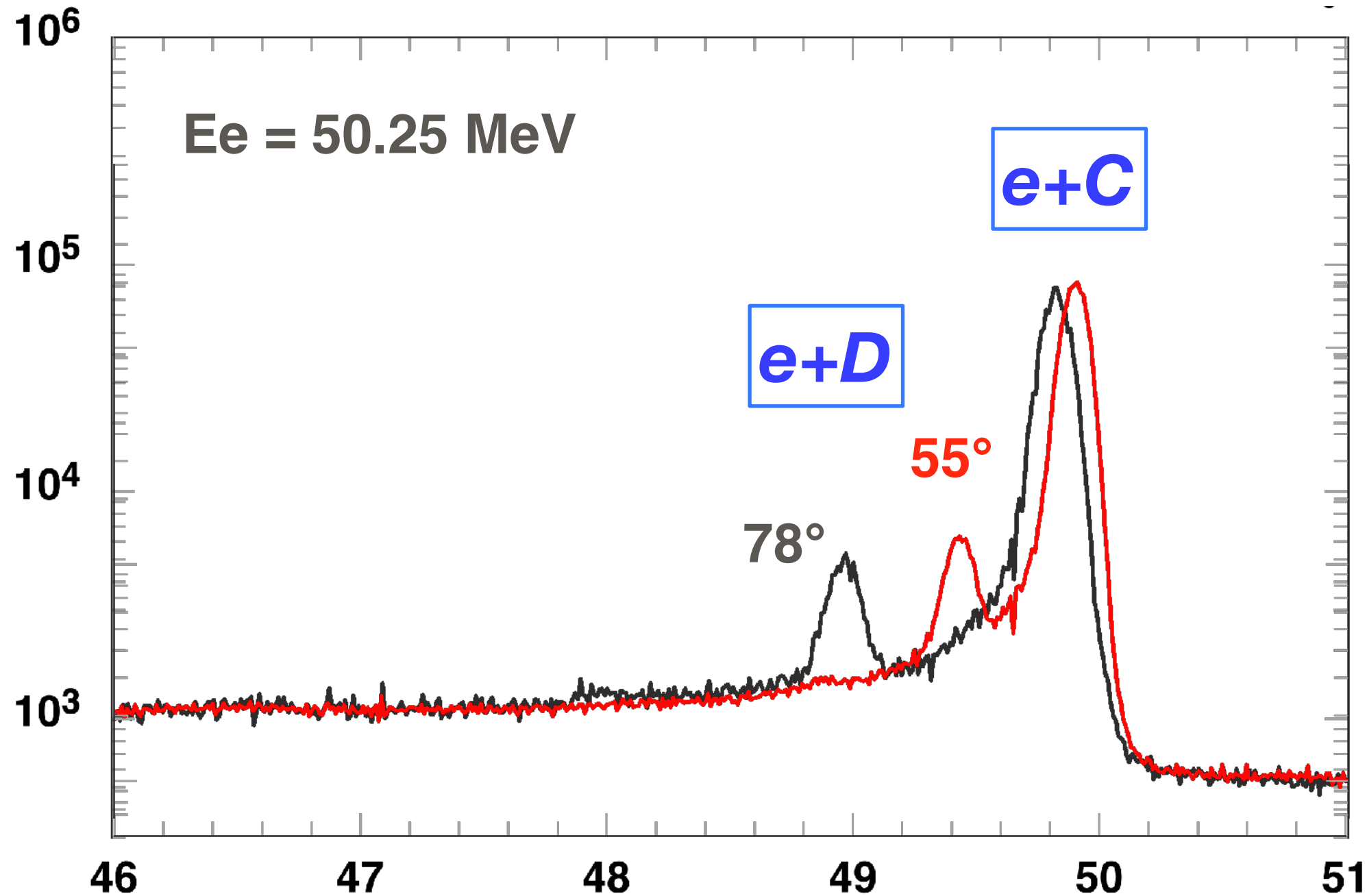
Low-energy electron scattering provides $\langle r^4 \rangle$

charge form factor at low q

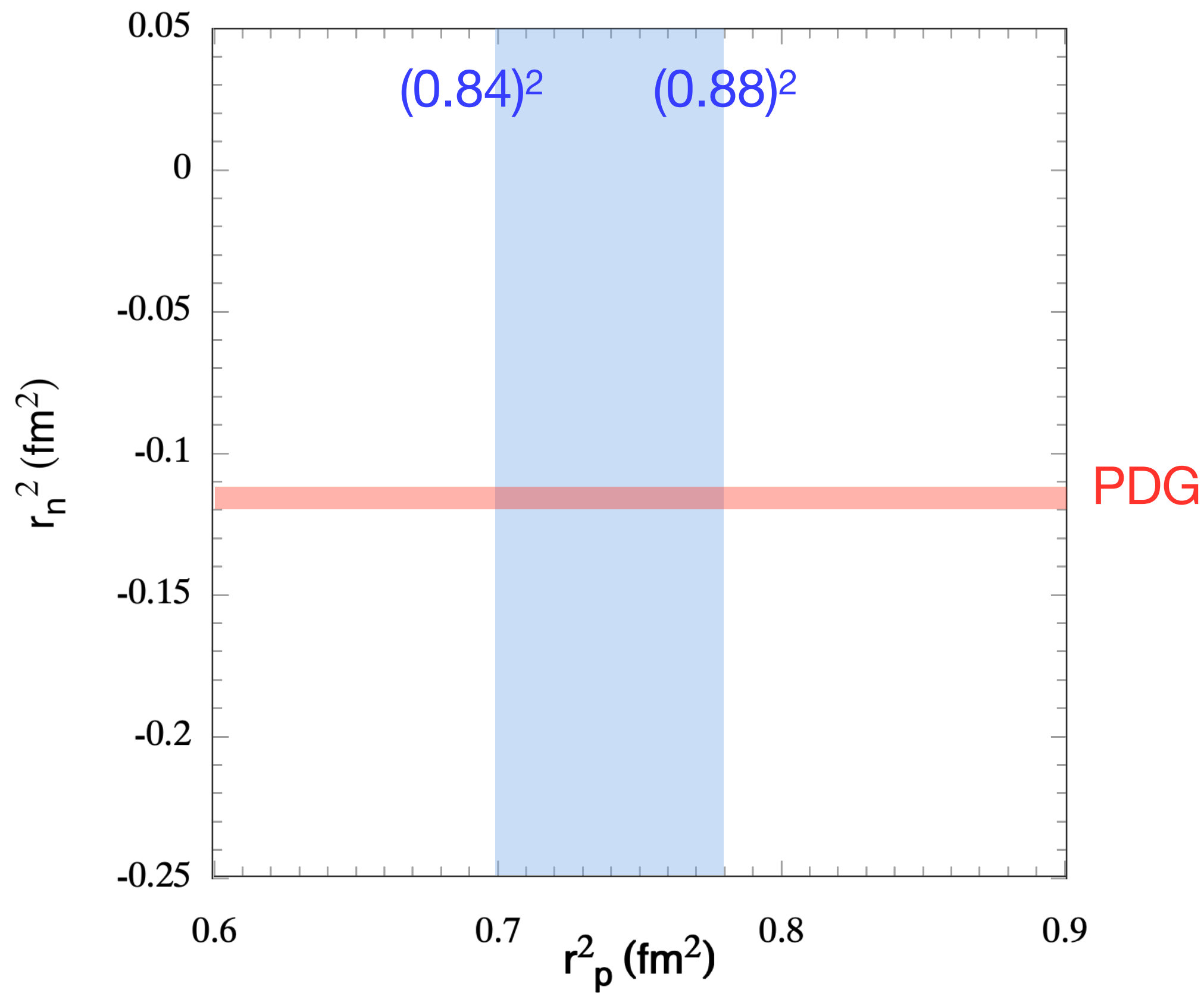
$$G_{C0} \sim 1 - \frac{\langle r_c^2 \rangle}{3!} Q^2 + \frac{\langle r_c^4 \rangle}{5!} Q^4 - \dots$$

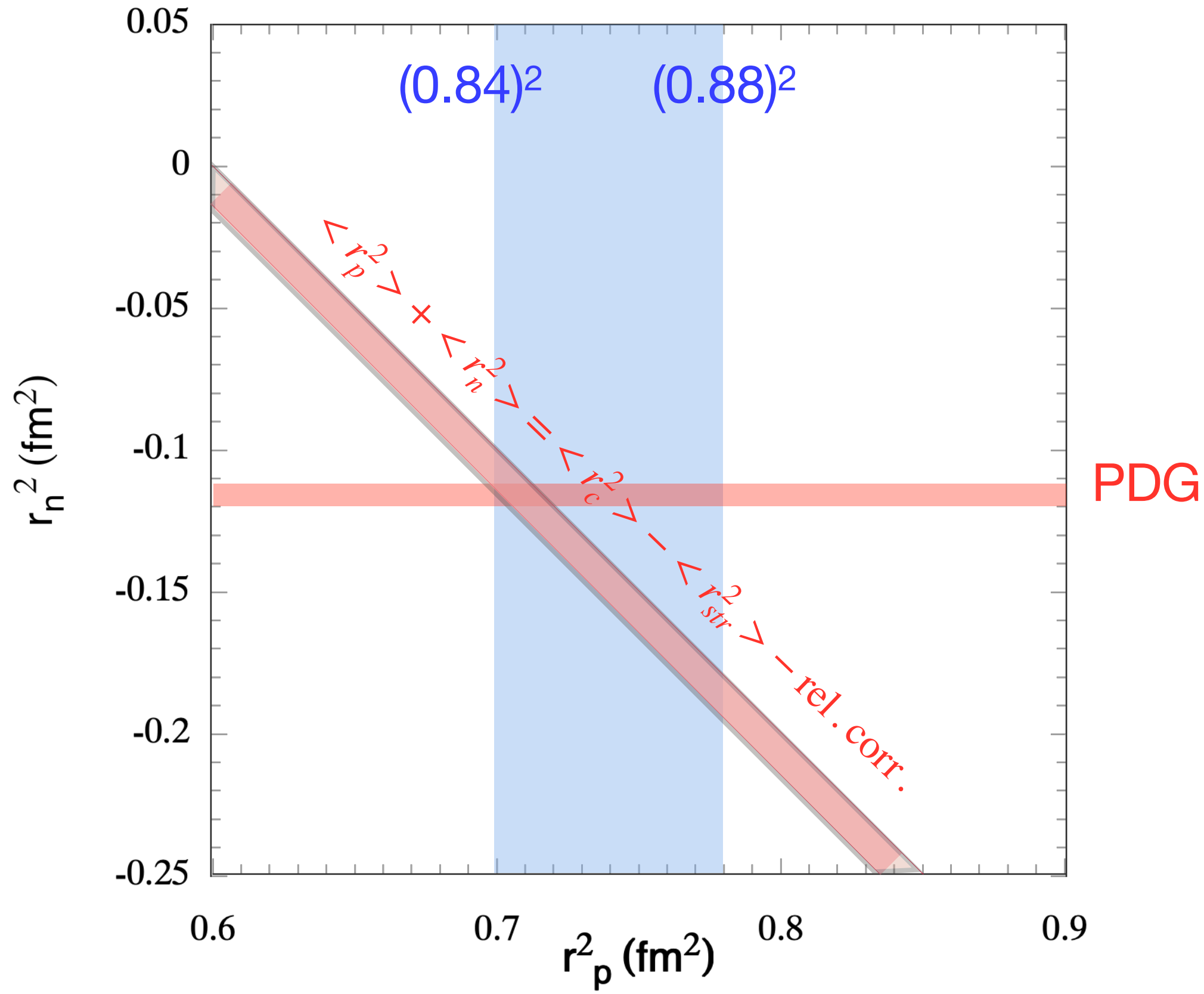


First shots of CD2(e,e') @ ULQ2

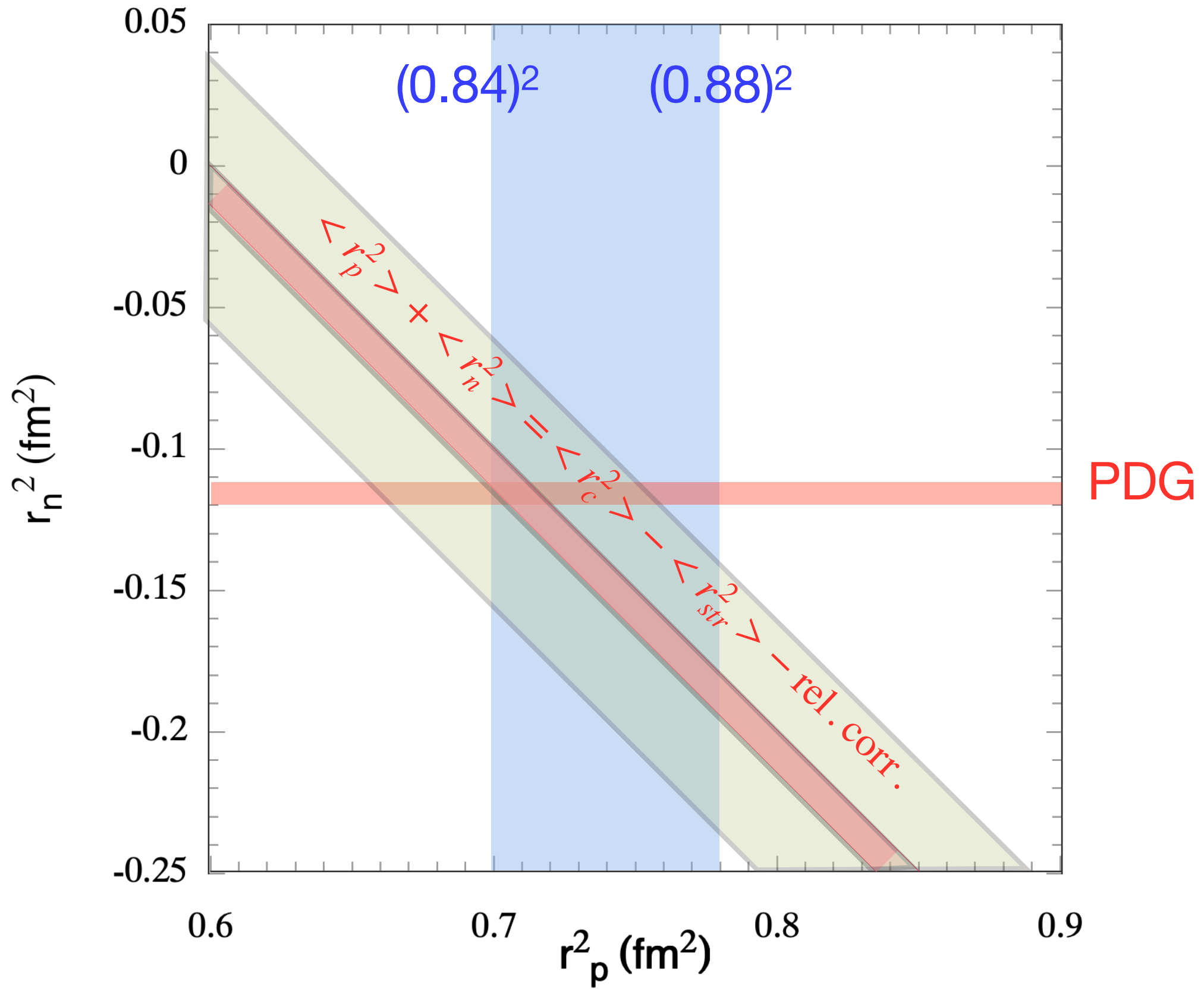


a series of CD2 measurements is underway





$$\langle r_c^4 \rangle = \langle r_{p(point)}^4 \rangle + \frac{10}{3} \langle r_{p(point)}^2 \rangle (\langle r_p^2 \rangle + \langle r_n^2 \rangle) + \text{rel. corr.}$$



conclusions

- low-q e-scattering activities in Japan
Tohoku ULQ2 for proton radius etc.
RIKEN SCRIT for structure studies of exotic nuclei
- Tohoku ULQ2 (Ultra-Low Q2)
 $E_e = 10 - 60 \text{ MeV}$
 $\theta_e = 30 - 150 \text{ deg.}$
high-resolution twin spectrometers
 $Q^2 = 3 \times 10^{-5} - 0.013 (\text{GeV}/c)^2$: lowest-ever
- CH2(e,e') proton radius will be available this year
CD2(e,e') this year

conclusions

- low-q e-scattering activities in Japan
Tohoku ULQ2 for proton radius etc.
RIKEN SCRIT for structure studies of exotic nuclei
- Tohoku ULQ2 (Ultra-Low Q2)
 $E_e = 10 - 60 \text{ MeV}$
 $\theta_e = 30 - 150 \text{ deg.}$
high-resolution twin spectrometers
 $Q^2 = 3 \times 10^{-5} - 0.013 (\text{GeV}/c)^2$: lowest-ever
- CH2(e,e') proton radius will be available this year
CD2(e,e') this year

We plan to organize a workshop in Sendai, Japan, on

“Low-Energy Electron Scattering for Nucleon and Exotic Nuclei”

Date : Oct. 28 - Nov. 1, 2024

Place : Sendai